https://doi.org/10.5194/egusphere-2025-2734
Preprint. Discussion started: 27 June 2025

A multiple spatial scales water use simulation for capturing its spatial heterogeneity through cellular automata model

Jiayu Zhang[a], Dedi Liu*[,a,b,c], Jiaoyang Wang[a], Feng Yue[a], Hanxu Liang[a], Zhengbo Peng[a], Wei Guan[a]

[a] State Key Laboratory of Water Resources Engineering and Management, Wuhan University, Wuhan, China

[b]Hubei Provincial Key Lab of Water System Science for Sponge City Construction, Wuhan University, Wuhan, China

[c] Department of Earth Science, University of the Western Cape, Robert Sobukwe Road, Bellville 7535, Republic of South Africa

* Correspondence to: Dedi Liu: dediliu@whu.edu.cn

https://doi.org/10.5194/egusphere-2025-2734
Preprint. Discussion started: 27 June 2025

Abstract: Reliable water use simulation is essential for sustainable water resource planning, especially under intensifying pressures from climate change, population growth, and socio-economic transitions. While previous studies have extensively explored water availability as supply side modeling across multiple spatial scales for its spatial heterogeneity, the water demand side remains relatively underdeveloped—often constrained by fixed spatial scales and coarse statistical data that assume spatial homogeneity. This mismatch between supply side and demand side limits the ability of existing models to accurately represent spatial heterogeneity in water use and brings uncertainty into water resource allocation strategies. To address this mismatch, we propose a novel multi-scale water use simulation framework by integrating cellular automata (CA) model with Generalized Likelihood Uncertainty Estimation (GLUE). The CA model captures the spatial heterogeneity of water use through the grid-based update rules. Two update rules are adopted—probability rule (i.e., capturing stochastic transitions via distribution fitting) and linear rule (i.e., modeling neighborhood-weighted evolution). To evaluate the impacts of spatial scale on water use heterogeneity, simulations are conducted at three spatial scales: 1 km, appropriate scale, and prefecture scale across 341 prefectures in China. Results show that both the update rule and spatial scale significantly affect spatial heterogeneity and uncertainty of water use. The probability rule can capture the broader variability but results in higher Root Mean Squared Error (*RMSE*) and Relative Error (*RE*) while the linear rule brings more stable performance with lower errors. While the 1 km scale increases uncertainty due to sensitivity to local fluctuations, and the prefecture scale suppresses spatial details, the appropriate scale offers the best trade-off between stability and spatial heterogeneity. The uncertainty quantified by GLUE, expresses as confidence intervals, varies across prefectures and spatial scales. Overall, the proposed framework offers a flexible tool for multi-scale water use simulation and highlights the critical role of spatial heterogeneity, thereby supporting adaptive water resource planning and management.

https://doi.org/10.5194/egusphere-2025-2734
Preprint. Discussion started: 27 June 2025

Key words: demand-side water modeling; spatial scale; water resources management; water scarcity assessment

https://doi.org/10.5194/egusphere-2025-2734
Preprint. Discussion started: 27 June 2025

1 Introduction

Water scarcity has become one of the most pressing global challenges, exacerbated by climate change, population growth, and unsustainable water use practices (Avargani et al. 2022, Huang et al. 2021, Kaewmai et al. 2019, Rosa et al. 2020). Nearly 2.3 billion people is living in regions facing water scarcity (Brunner et al. 2019, Dolan et al. 2021, Mekonnen and Hoekstra 2016). In this context, accurate and timely assessments of water scarcity are essential for effective water management, resource allocation, and policy-making (Avargani et al. 2022, Cao et al. 2018). A scientifically rigorous water scarcity assessment requires a comprehensive understanding of both available water resources and water use (Brunner et al. 2019, Ji et al. 2025, Sun et al. 2022). However, these two components are often represented at incompatible spatial scales, resulting in mismatches that complicate accurate evaluation and integrated water resources planning (Almino and Rufino 2021, Kang et al. 2017).

In the past few decades, significant advancements in hydrological modeling, satellite remote sensing, and reanalysis datasets have enabled researchers to simulate surface and ground available water resources across various temporal and spatial scales—from daily basin-scale runoff forecasts to long-term continental water balance projections (Horta et al. 2024, Su et al. 2024, Yang et al. 2021, Zhang and Long 2021). These advancements have laid the foundation for widely used tools such as SWAT, VIC, H08, and PCR-GLOBWB, which help water managers better understand available water resources under different spatial-temporal scales (Hersbach et al. 2020, Kovacevic et al. 2020, Noori and Kalin 2016, Sunkara and Singh 2022). Though there has been water use simulation progress, it still faces significant challenges and has yet to achieve the same spatial level of sophistication as the simulation of available water resources. The primary limitations of water use simulation lies in the available spatial scales of water use data (Hou et al. 2024, Zhang et al. 2023). Much of the existing researches rely on a coarse, aggregated dataset such as national statistics, sectoral usage reports,

https://doi.org/10.5194/egusphere-2025-2734
Preprint. Discussion started: 27 June 2025

or administrative boundaries (e.g., counties, provinces) (Carvalho et al. 2021, Wu et al. 2022, Zhang et al. 2023). These datasets inherently assume uniform water use within each administrative unit, and often overlook the spatial heterogeneity of water use. This oversimplification limits the ability of water use simulations to capture spatial variation, particularly in regions with pronounced heterogeneity (Brunner et al. 2019, Su et al. 2024).

Simulating water use at a grid scale provides a promising solution to address the spatial scale mismatch, allowing for a more accurate representation of water use dynamics and capturing regional variations (Su et al. 2024, Wu and Lu 2021). A grid-based approach allows for a more accurate representation of water use dynamics by capturing fine-scale spatial heterogeneity, which administrative survey data often overlook. Zhang et al. (2023) integrated the Iterative Input Selection algorithm with Convolutional Neural Networks to simulate annual irrigation water use, producing high-resolution grid maps with a spatial resolution of 1 km for mainland China. Hou et al. (2024) developed a monthly dataset on industrial water withdrawals, incorporating spatial resolutions of 0.1° and 0.25° by utilizing enterprise data, product yields, and water use statistics. These studies have demonstrated that the downscaled water use data from administrative level to grid scale can catch a more detailed and region-specific representation of water use patterns, thereby improving their applicability in water resource management and water scarcity assessment. However, these studies still rely on a fixed spatial grid scale, limiting their ability to capture the full spatial heterogeneity of water use. The effects of spatial resolution on the representation of water use heterogeneity remain insufficiently explored. In particular, finer scales (such as 1 km grids) can capture localized variations in water use, coarser scales (such as regional or administrative boundaries) tend to smooth over spatial differences, potentially obscuring critical patterns (Luo et al. 2020, Sun et al. 2022). Therefore, simulating water use across multiple spatial scales is essential for capturing the full spectrum of spatial heterogeneity. By incorporating the results at different spatial scales,

https://doi.org/10.5194/egusphere-2025-2734
Preprint. Discussion started: 27 June 2025

this simulation can account for the fine-scale dynamics of water use in urban, agricultural, and industrial areas more effectively, offering a comprehensive understanding of water use patterns and improving the accuracy of water scarcity assessments (Su et al. 2024, Sunkara and Singh 2022).

Since the spatial scale of water use simulation depends on the spatial scale of the input data (Horta et al. 2024, Sharifi et al. 2021, Zhang et al. 2023), achieving multi-scale water use simulation requires a model that can flexibly handle different input spatial scales. Such a model should be adaptable to varying spatial resolutions and ensure accurate simulation of water use, whether the focus is on fine-scale urban areas, intermediate regional levels, or broader national assessments. The cellular automata (CA) model, with its grid-based structure, offers a suitable framework for spatially explicit modeling across multiple scales by adjusting both the spatial resolution of input data and the design of updating rules (Al-Shaar et al. 2022, Sapino et al. 2023, Tariq et al. 2023, Wang et al. 2020). The CA model can thus be employed to support multi-scale water use simulation. And as uncertainties are inherently associated with the selection of spatial scales and update rules (Yin et al. 2020, Zhang and Long 2021), it is critical to quantify and address these uncertainties to ensure the reliability of simulation outcomes.

The aim of this research is to develop a multi-scale water use simulation framework that specifically addresses the impact of spatial scale on the spatial heterogeneity of water use. The framework is mainly composed of the CA model for simulating water use dynamics across various spatial scales and an uncertainty analysis technique for quantifying the uncertainties of the simulation. The proposed framework will not only facilitate a deeper understanding of the influences of spatial scale on water use heterogeneity in diverse regions, but also improves the accuracy of water scarcity assessments and supports more effective resource management. Ultimately, the proposed framework contributes to advancing sustainable water governance in areas facing pronounced water stress.

https://doi.org/10.5194/egusphere-2025-2734
Preprint. Discussion started: 27 June 2025

2. Methodology

To develop a multi-scale water use simulation model, the dynamic spatial scale simulation capabilities of the CA model should be firstly leveraged. The particularly advantage of CA model is modeling complex global dynamics through simple local interactions and transition rules (Al-Shaar et al. 2022, Liu et al. 2021, Tariq et al. 2023). Moreover, the grid-based structure of the CA model allows it to flexibly accommodate various spatial resolutions, making it well-suited for modeling water use at multiple spatial scales (Sapino et al. 2023, Wang et al. 2020). In this framework, water use grid maps at different spatial scales are first prepared as inputs to the CA model. Each grid is treated as an individual cell in the CA model, with the water use amount at each cell representing its state. Based on the neighborhood configuration and the initial baseline year water use data, water use values for future years are simulated using predefined update rules for each cell at multiple spatial scales. The procedure of our proposed CA model for multi-scale water use simulation is depicted in Figure 1.

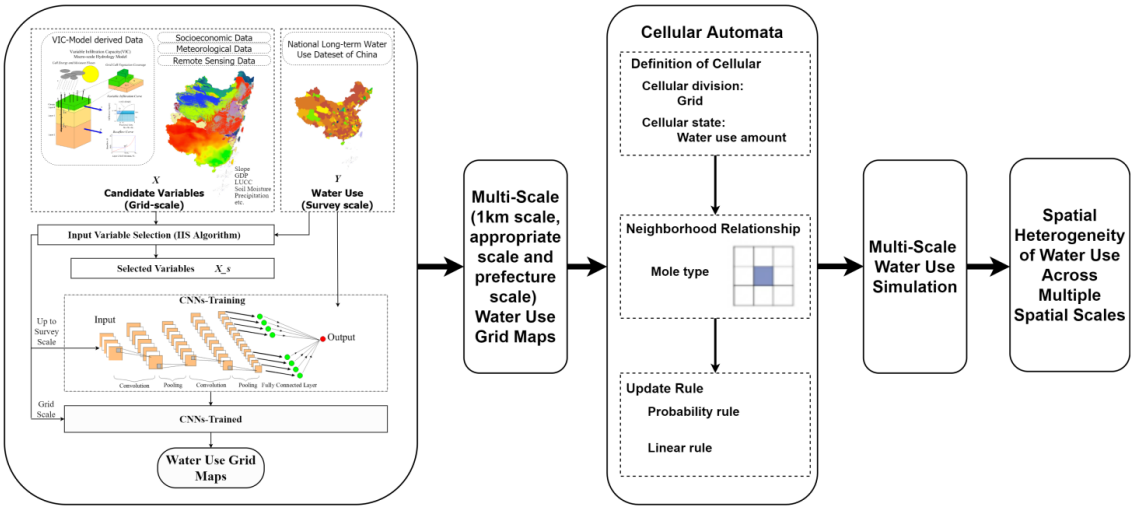

Figure 1. Procedure of the multi-scale water use simulation

To capture the spatial heterogeneity of water use dynamics at different scales, the Coefficient of Variation

https://doi.org/10.5194/egusphere-2025-2734
Preprint. Discussion started: 27 June 2025

(CV) (Abdi 2010) and Moran's I spatial autocorrelation index (Tiefelsdorf et al. 1995) are employed here. The CV measures the relative variability of water use across regions, with higher values indicating greater spatial heterogeneity. Moran's I assesses the degree of spatial autocorrelation, identifying whether similar values are spatially clustered (positive values) or dispersed (negative values). These two indices are applied to evaluate the spatial heterogeneity of water use grid maps at different spatial scales (i.e., 1 km, appropriate scale, and prefecture scale), and figure out the influences of the spatial variations on water use dynamics and uncertainty in the simulation results.

To quantify the uncertainties of water use simulation for providing a more robust foundation for water scarcity assessment and policy-making (He et al. 2018, Knox et al. 2018, Sharifi et al. 2021), the Generalized Likelihood Uncertainty Estimation (GLUE) method is adopted here. GLUE provides a probabilistic framework for model evaluation by exploring a wide range of parameter sets and assigning likelihoods to each based on their performance. This approach effectively addresses model equifinality—where multiple parameter combinations yield similar outputs—and is particularly well-suited for complex, non-linear models such as cellular automata (Liu et al. 2015, Yin et al. 2020).

2.1 Water Use Grid Maps generating

The spatial scale of water use simulation is determined by the spatial scale of the input data, so water use grid maps at different spatial scales should be prepared as input to the simulation model. To obtain the water use grid maps, several steps should be done to convert the water use data at administrative survey scale into the varying spatially explicit scales. First, the water use data at administrative survey scale is processed and downscaled to grid-based formats by the iterative input selection (Galelli and Castelletti 2013) and Convolutional Neural Networks (CNN) algorithms. The iterative input selection algorithm is used to select the most relevant variables for water use, while the CNN model captures the relationships between input

https://doi.org/10.5194/egusphere-2025-2734
Preprint. Discussion started: 27 June 2025

variables and water use (Zhang et al. 2023). Next, the appropriate spatial scale for water use simulation is identified using an end-to-end deep learning-based spatial scale adaptive selection model (Liu et al. 2022, Zhang et al. 2025). Finally, water use grid maps are obtained at small spatial scale (e.g., 1km), and then the appropriate spatial scale and prefecture scale.

2.2 Cellular automata model for water use simulation

The CA model, grounded in complexity theory, is widely used in land use and urban growth modeling. It provides a robust platform for simulating spatial phenomena governed by local interactions and transition rules (Sapino et al. 2023, Tariq et al. 2023). Each cell in a CA model represents a discrete spatial unit that updates its state over time based on predefined rules and the states of its neighboring cells. It's decentralized, bottom-up modeling structure enables the simulation of complex global behaviors emerging from simple local dynamics (Al-Shaar et al. 2022, Wang et al. 2020). This model often employs two distinct update rules to simulate water use over time: the probability rule and the linear rule. Both rules account for spatial interactions between neighboring cells and allow for the simulation of water use at multi-scale, capturing the heterogeneity of water use across different geographical regions. By applying both rules independently, the effectiveness of update rules in simulating water use at multi-scale is assessed.

2.2.1 Probability rule in CA

The probability rule in the CA model is designed to capture the stochastic nature of water use transitions. The state of each grid cell (i.e., representing the amount of water use) is divided into k distinct intervals using equal-frequency categorization according to its historical data. This categorization ensures that the intervals reflect the variations in water use over time. For each interval, the most suitable statistical distribution is selected using the Akaike Information Criterion (AIC). The distribution is chosen from a set of candidate

https://doi.org/10.5194/egusphere-2025-2734
Preprint. Discussion started: 27 June 2025

distributions, including normal, lognormal, exponential, gamma, and uniform.

Once the most appropriate distribution is found for each interval, a state transition matrix is created based on the transition of states from one year to the next. The transition matrix indicates the probabilities of a grid cell's state transitioning to another state (i.e., another interval) in the following year. Using these transition probabilities, the model predicts which interval each grid cell's state will fall into at the next time step. A random sample is then drawn from the corresponding distribution of the predicted interval, providing a predicted water use value for the next time step. This approach introduces variability, reflecting the inherent randomness and uncertainty in future water use patterns.

In the probability rule, the calibrated parameter is the number of state intervals and is denoted as k. The value of k directly affects the granularity of the state categorization and the accuracy of the state transition matrix. A larger k increases the resolution of the state representation and captures the finer variations in water use, but a larger k can also lead to overfitting. And a smaller k oversimplifies the demand pattern. To calibrate the parameter k, the historical and observed water use data is divided into a calibration and a validation sets. And the performances of the model with different k values is then evaluated by the Root Mean Squared Error (*RMSE*) and Relative Error (*RE*) metrics. The optimal k can be calibrated by the minimums of the *RMSE* and *RE* in the validation period, ensuring a balance between model accuracy and generalizability.

2.2.2 Linear rule in CA

The linear rule in CA updates the water use of each cell according to the weighted average of its current state and the states of its neighboring cells. The linear rule assumes that the water use at a given grid cell is influenced by both its own previous state and the water use of adjacent cells. The linear rule is expressed as the Equation (1).

https://doi.org/10.5194/egusphere-2025-2734
Preprint. Discussion started: 27 June 2025

$$W(t+1) = \alpha W(t) + \beta \sum_{i=1}^{n} \omega_i W_i(t) \quad (1)$$

where $W(t+1)$ is the predicted water use of the central cell at time $t+1$, $W(t)$ is the current water use of the central cell at time t, $W_i(t+1)$ represents the water use at the i^{th} neighboring cell ($i=1,2,\ldots,8$) at time t, ω_i is the weight that is assigned to the i^{th} neighboring cell, α and β are coefficients that control the relative influence of the central cell's own water use and the neighboring cells' water use.

To accurately capture the influences of neighboring cells, the weight ω_i for each neighboring cell is determined by an inverse distance weighting scheme with an exponential decay and is expressed as the Equation (2).

$$\omega_i = \frac{1}{d_i^p} \quad (2)$$

where d_i is the Euclidean distance between the central cell and the i^{th} neighboring cell, p is an adjustable exponent that controls the rate of decay in the influence of neighboring cells.

To determine the parameters α, β, and p, the observed period is also divided into a calibration period and a validation period. After the model runs with different parameter combinations, and their performances are assessed in terms of *RMSE* and *RE*, the optimal parameter set will be picked out by the minimum of the performance metrics in the validation period.

2.3 Generalized Likelihood Uncertainty Estimation for water use simulation

Generalized Likelihood Uncertainty (GLUE) is a probabilistic approach that evaluates a model's performance by considering a wide range of plausible parameter sets and quantifying the likelihood of each set in its ability to reproduce observed data (Chen et al. 2011, Sharifi et al. 2021, Taormina et al. 2016). Unlike traditional deterministic calibration methods, GLUE acknowledges the inherent equifinality in environmental modeling that also is the possibility of the acceptable results from the multiple parameters set. The GLUE is

https://doi.org/10.5194/egusphere-2025-2734
Preprint. Discussion started: 27 June 2025

incorporated into the CA model to assess the uncertainty in water use simulations.

The GLUE is applied in both the probability rule and the linear rule of the CA model to evaluate the uncertainty of water use simulations. There are six steps. (1) Parameter Selection: the number of state intervals k for the probability rule, and the self-influence coefficient α, the neighboring influence coefficient β, and the distance decay exponent p for the linear rule; (2) Parameter Sampling: a large number of parameter sets are generated by the uniform sampling within specified ranges for each parameter; (3) Model Simulation: the CA model is executed by each parameter set to simulate water use for the target period; (4) Likelihood Estimation: *RMSE* and *RE* values are calculated for each simulation to evaluate how well the simulated results match the observed data; (5) Behavioral Parameter Identification: behavioral parameter sets can yield acceptable likelihood values according to the thresholds that is determined by the calibration data; (6) Uncertainty Quantification: from the range of outputs from the behavioral parameter sets, a prediction interval is constructed quantify the uncertainty associated with the water use projections.

2.4 Spatial Heterogeneity of water use

To comprehensively understand the variability and spatial relationships of water use patterns across different spatial scales, Coefficient of Variation (CV) (Abdi 2010) and Moran's I (Tiefelsdorf et al. 1995) are used to analyze the spatial heterogeneity of water use. CV is defined as the ratio of the standard deviation to the mean of water use values at each spatial scale, offering a normalized measure of dispersion. It is a primary indicator used to quantify variability in water use across grid cells (Canchola et al. 2017). A higher CV value indicates greater spatial variation in water use, while a lower CV suggests more uniform water use patterns across the region. Once the CV for each grid cell is calculated, the extent of water use spatial heterogeneity is assessed, and areas with high variability are identified as more susceptible to water stress and fluctuations in demand (Botta-Dukát 2023, Liu et al. 2020).

https://doi.org/10.5194/egusphere-2025-2734
Preprint. Discussion started: 27 June 2025

Moran's I can reflect the spatial autocorrelation by measuring the degree to which one grid cell's water use is similar to that of neighboring grid cells. Moran's I provides an overall measure of spatial dependence, where a positive Moran's I indicates a clustering of similar water use values (either high or low) in neighboring grid cells, while a negative Moran's I suggests a dispersed pattern. A value close to zero indicates a random spatial pattern with no significant clustering (Gedamu et al. 2024, Shortridge 2007). By calculating Moran's I across different spatial scales, we are able to detect whether water use patterns exhibit spatial clustering or they are more randomly distributed. Moran's I can therefore help us understand the regional patterns of water use and identify areas that require targeted management interventions (Fu et al. 2024, Yamada 2024).

Both the CV and Moran's I provide a robust framework to analyze spatial heterogeneity in water use. The CV provides a measure of variability, while Moran's I reveals the extent of spatial correlation in water use. They offer a more comprehensive understanding of the spatial dynamics across different regions.

3 Study area and datasets

3.1 Study Area

Situated on the northwestern shore of the Pacific Ocean, China boasts vast territory, a large population, and diverse climate conditions (Ji et al. 2025, Sun et al. 2022). Over the years, the volume of water use in China has surged significantly rising from 3305 km^3 in 1965 to 5925 km^3 in 2024 (Ji et al. 2025). Owing to the country's varied climate conditions and pronounced spatiotemporal heterogeneity of water resources, water scarcity has become a recurrent challenge, exacerbated by the looming threats of climate change and rapid socio-economic development (Hou et al. 2024, Wang et al. 2021). Notably, China is expected to experience greater impacts from climate change than the global average (Kang et al. 2017, Sun et al. 2022, Yan et al. 2019). Therefore, conducting a multi-scale water use simulation study in China is particularly meaningful due

https://doi.org/10.5194/egusphere-2025-2734
Preprint. Discussion started: 27 June 2025

to the country's complex water resource challenges, amplified by regional disparities, climate change, and rapid socio-economic development. China comprises 31 provincial-level administrative divisions, including provinces, autonomous regions, and municipalities. As outlined in the study by Zhou et al. (2020), the administrative divisions are categorized at the prefecture level, totaling 341 prefectures (Figure. 2).

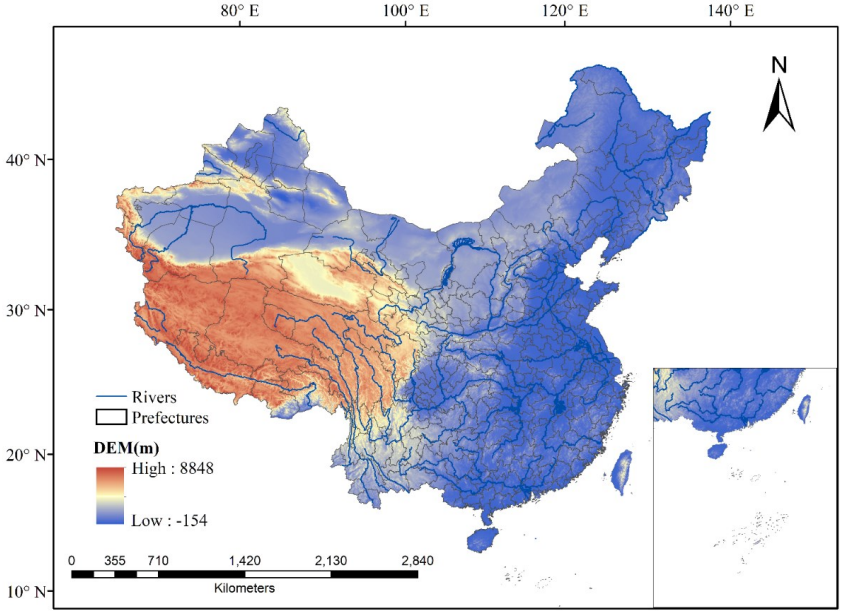

Figure. 2 Prefectures and major rivers in study area

3.2 Datasets and Preprocessing

To obtain water use grid maps, the observed datasets related to irrigation water use, domestic water use, and industrial water use were collected. The observed datasets are composed of the annual water use statistical survey data at the administrative scale, soil moisture data derived from hydrological models, socio-economic data like *GDP* (Gross Domestic Product) and population, meteorological data from point observations, and satellite remote sensing data including the normalized difference vegetation index (*NDVI*) and night light data.

Various spatial interpolation and downscaling methods are employed to transform the datasets into

https://doi.org/10.5194/egusphere-2025-2734
Preprint. Discussion started: 27 June 2025

different spatial scales. To simulate water use at different spatial scales, we transform the spatial scale of the dataset to 1km, appropriate spatial scale (Zhang, et al., 2025) and prefecture scale. The details of the transform methods can be found in the reference of Zhang et al. (2023). Nighttime light remote sensing data is also combined with the land use information to perform upscaling or downscaling at spatial scales (Ye et al. 2021).All the adopted datasets and their corresponding preprocessing methods are listed in Table 1.

Table 1. Datasets and corresponding preprocessing methods

Variables	Data Sources	Origin Data Format	Origin Resolution	Processing Method
Precipitation (P)	CMA*	Point observation	\	Interpolation (ANUSPLIN)
Temperature (T)	CMA*	Point observation	\	Interpolation (IDW)
LUCC	RESDC**	Grid	30 m × 30 m	Upscale (Resample)
NDVI	RESDC**	Grid	1 km × 1 km	Upscale/downscale (Resample)
GDP	RESDC**	Grid	1 km × 1 km	Upscale/downscale (Resample)
Population	RESDC**	Grid	1 km × 1 km	Upscale/downscale (Resample)
DEM	SRTM	Grid	1 km × 1 km	Upscale/downscale (Resample)
Potential Evapotranspiration (PET)	\	\	\	P-M Equation/Interpolation (IDW)
Soil moisture (SM)	GDFC*** (He and Sheffield 2020)	NetCDF	0.25° × 0.25°	Downscale (Machine learning)(Guevara and Vargas 2019)
Night light (N-L)	DMSP-OLS	Grid	2.7 km × 2.7km	Upscale/downscale (Resample)
National Long-term Water Use Dataset of China	FigShare-PNAS(Zhou et al. 2020)	Excel	\	\

CMA*: China Meteorological Administration (http://data.cma.cn/); RESDC**: Resource and Environment Science and Data Center (https://www.resdc.cn/).

GDFC***: Global Drought and Flood Catalogue (http://hydrology.princeton.edu/data).

https://doi.org/10.5194/egusphere-2025-2734
Preprint. Discussion started: 27 June 2025

4. Results

4.1 Water use simulation by CA model

4.1.1 Water use simulation from the probability rule CA model

As the AIC can balance the model fitness and complexity by penalizing the number of parameters to prevent overfitting, it has been widely applied in probability distributions selection. Here, the AIC is employed to determine the most suitable probability distributions for water use grids across various prefectures. And the optimal probability distributions of water use grid at three different scales (i.e., 1km scale, appropriate spatial scale and prefecture scale) are identified as illustrated in Figure 3.

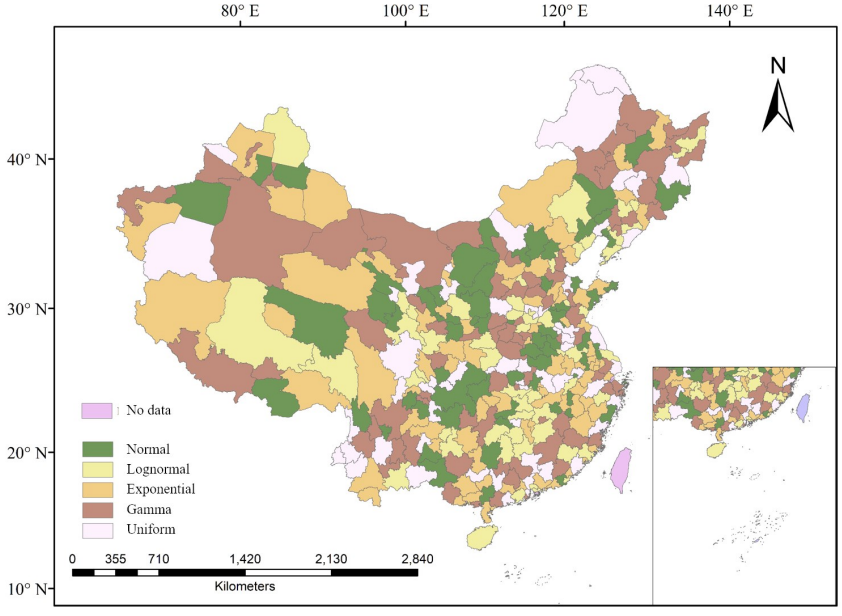

(a)

https://doi.org/10.5194/egusphere-2025-2734
Preprint. Discussion started: 27 June 2025

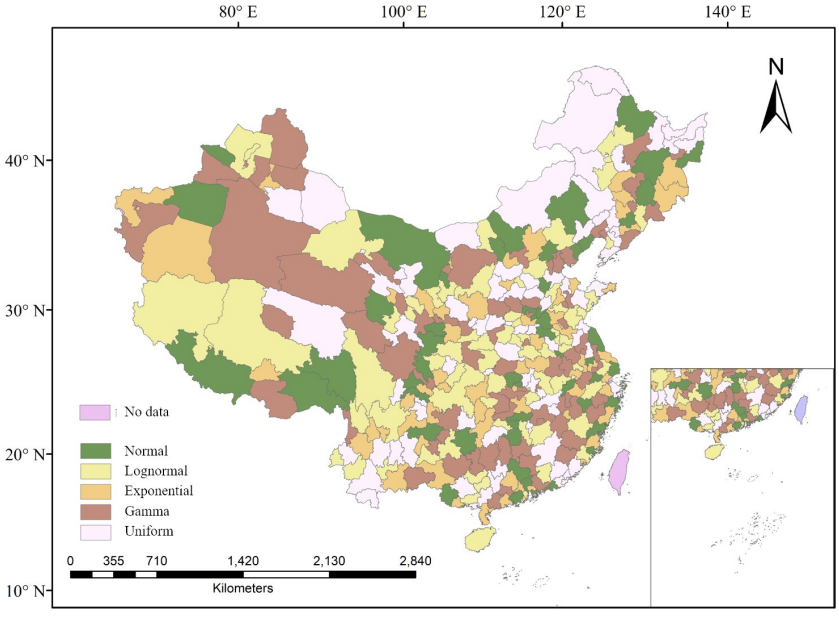

(b)

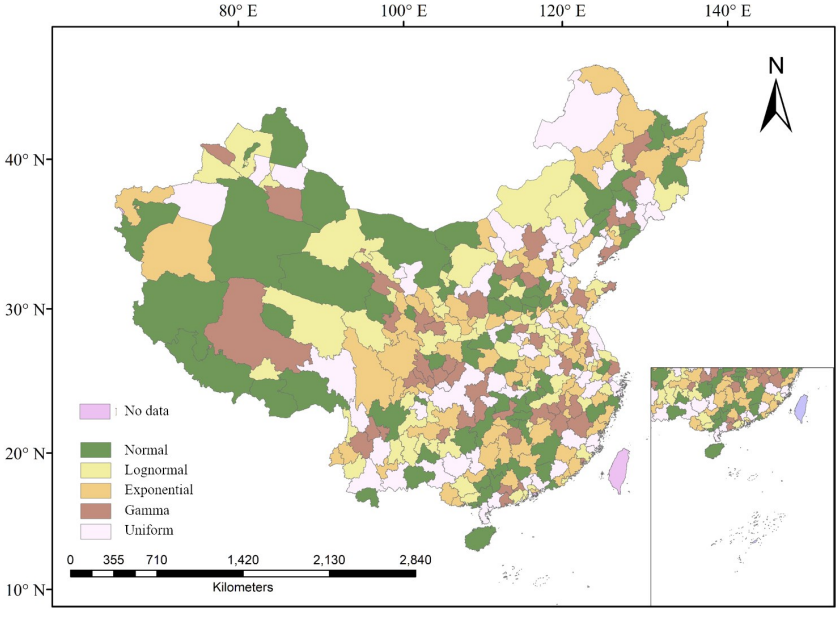

(c)

Figure. 3 Probability distribution types of water use at three spatial scales: (a) 1km scale; (b) appropriate spatial scale; (c) prefecture scale

https://doi.org/10.5194/egusphere-2025-2734
Preprint. Discussion started: 27 June 2025

The optimal probability distributions of water use grid maps across three spatial scales (i.e., 1 km scale, appropriate spatial scale, and prefecture scale) were identified and shown in Figure 3. The distribution types of water use reflect the underlying dynamics of water use at various scales. At the 1 km scale (as shown in Figure 3 (a)), most areas show a predominance of normal and log-normal distributions (i.e., in green and light yellow), indicating more stable and symmetric water use patterns. Water use in these areas are consistent with relatively socio-economic and climatic conditions, where are less fluctuated. However, the water use distributions are more frequently exponential or gamma (i.e., in light orange and brown) in areas with rapidly urbanization or industrialization in the central and eastern parts of China. And thus, water use are higher variability and stochasticity. The distribution types of water use at the appropriate spatial scale (as shown in Figure 3(b)) are similar with those at 1 km scale as shown in Figure 3 (a). More exponential and gamma distributions can be found in the significant agricultural activity areas at the appropriate spatial scale due to the irregular water use patterns driven by seasonal fluctuations and economic activities. When the spatial scale is up from 1 km to the appropriate ones, more nuanced understanding of water use dynamics can capture the impacts of local factors such as crop irrigation and industrial processes. Although the exponential distribution are found to be one of the prevalent types in regions with irregular or rapidly changing water use patterns at the prefecture scale as shown in Figure 3 (c), uniform and gamma distributions have appeared more frequently at this bigger prefecture scale. The transition to coarser spatial resolution leads to reduced spatial variability in water use, and the heterogeneity of water use is potentially oversimplified.

Based on the historical water use record from 1998 to 2013, a transition matrix at a grid cell can be determined to represent the probability of transition from the current state to its following time. According to the transition matrixes for each grid cell, the interval for the next state can be predicted. A random sample is then drawn from the predicted interval to obtain the predicted water use value for the following year. To

https://doi.org/10.5194/egusphere-2025-2734
Preprint. Discussion started: 27 June 2025

309 generate the simulated water use, the probability rule is applied at three different spatial scales (i.e., 1 km,

310 appropriate scale, and prefecture scale), and their results are shown as Figure 4.

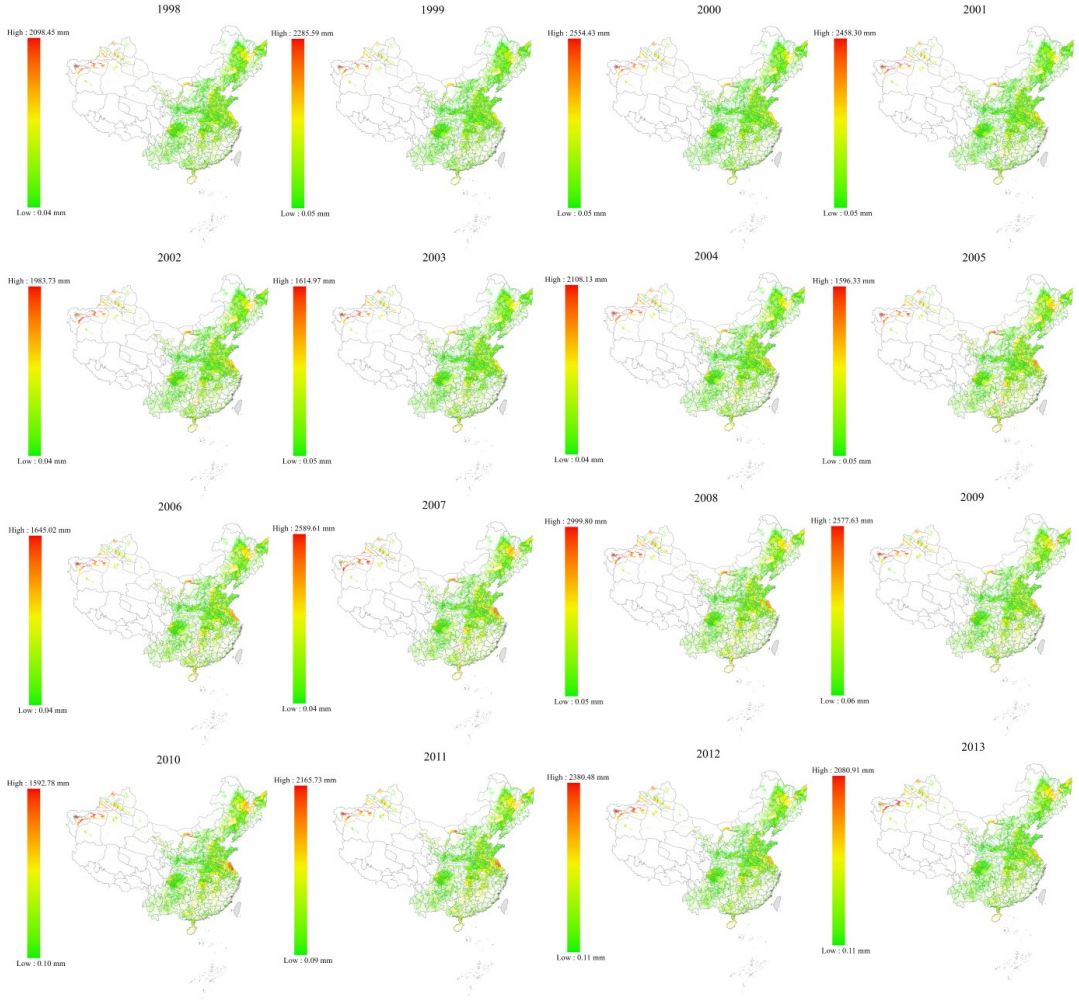

311

312 (a)

https://doi.org/10.5194/egusphere-2025-2734
Preprint. Discussion started: 27 June 2025

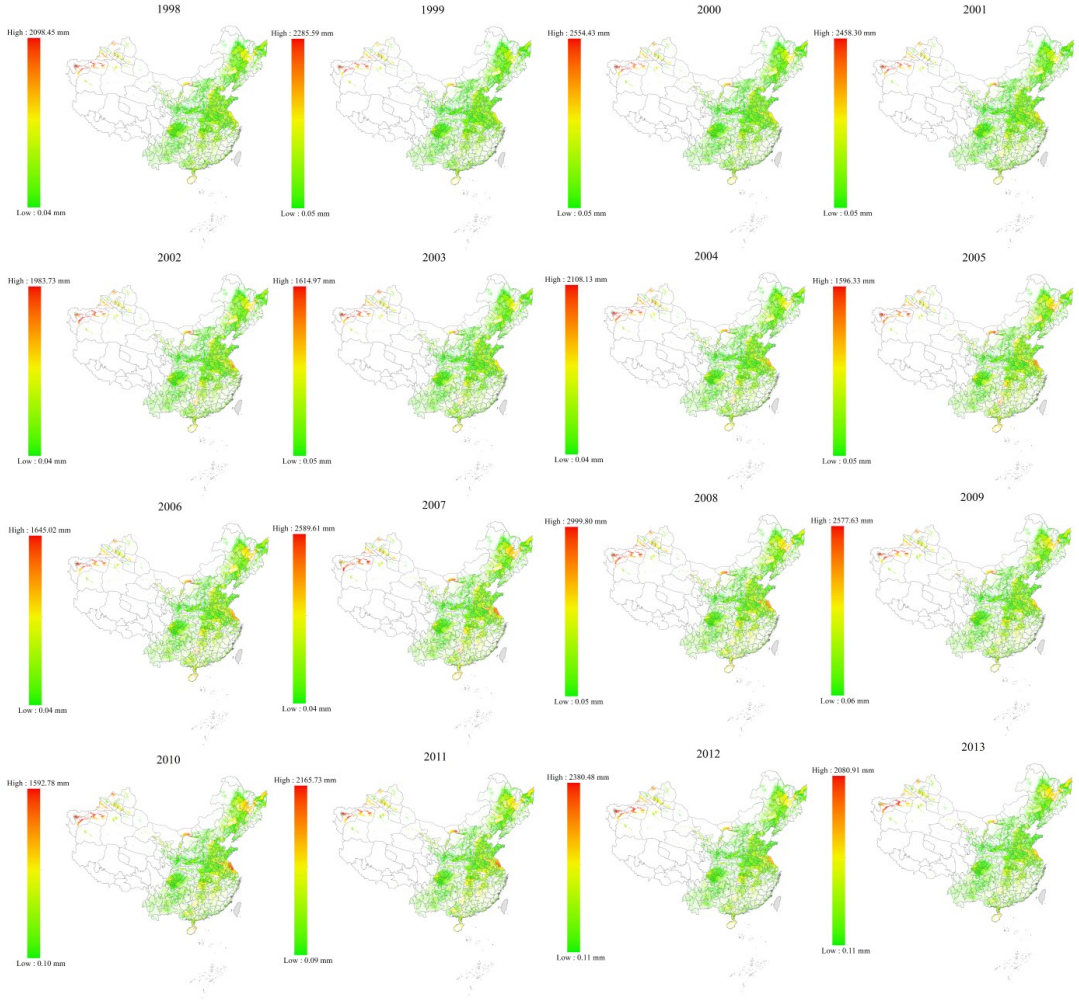

(b)

https://doi.org/10.5194/egusphere-2025-2734
Preprint. Discussion started: 27 June 2025

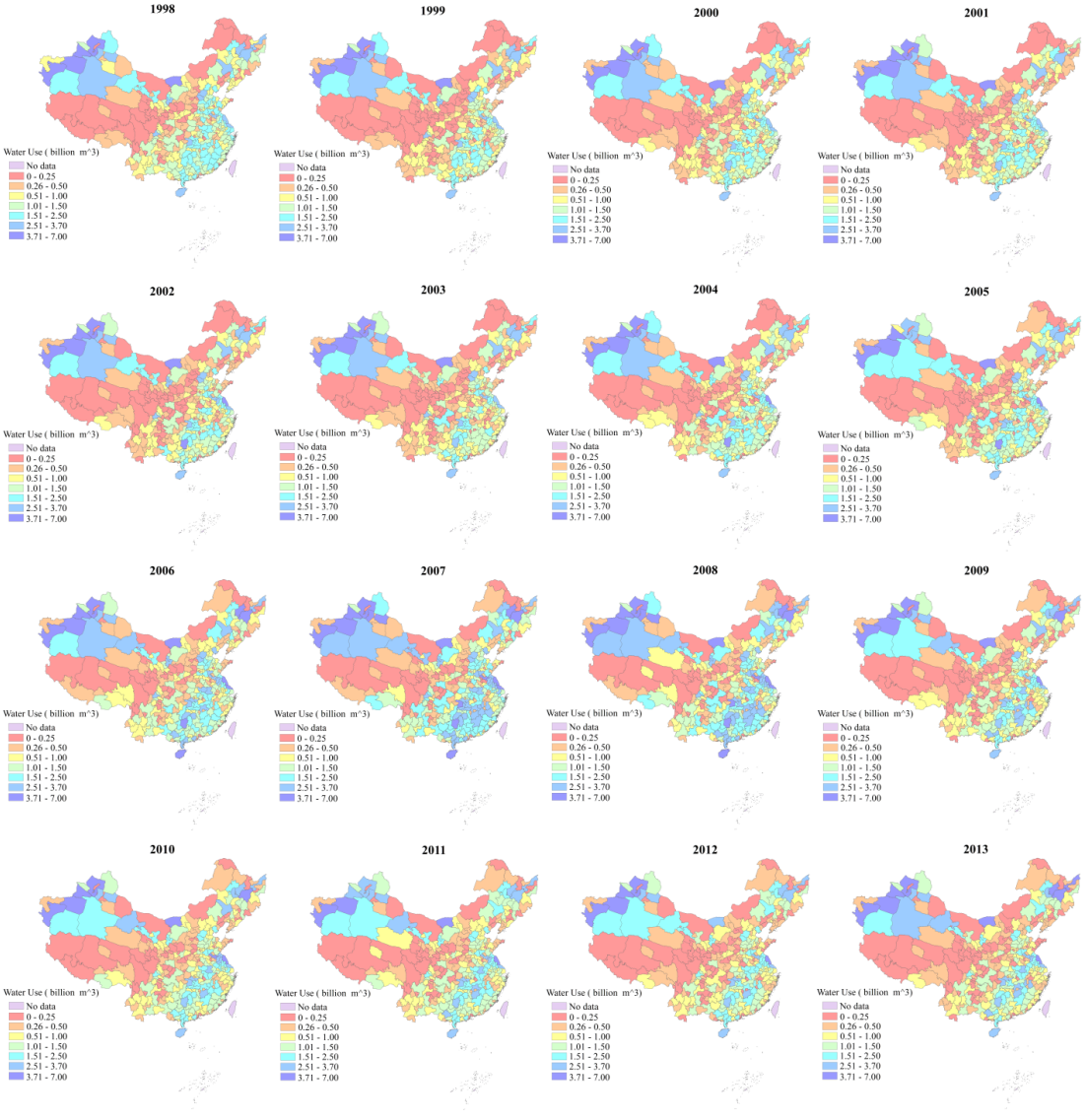

(c)

Figure. 4 Water use simulation results from the probability rule at three different scales: (a) 1km scale; (b) appropriate spatial scale; (c) prefecture scale

Water use simulation maps from 1998 to 2013 through the probability rule, has clearly highlight the spatial and temporal heterogenic at different spatial scales. The maps reveal the local increases in water use at the 1 km scale (as shown in Figure 4 (a)), particularly in major metropolitan areas in eastern and central parts

https://doi.org/10.5194/egusphere-2025-2734
Preprint. Discussion started: 27 June 2025

of China. These increases can be found across the whole time of the selected series driven by the population growth, industrial expansion, and urbanization. The results at the appropriate spatial scale (as shown in Figure 4 (b)) are different from those at the 1 km scale, their local variations become more homogeneous and stationary. It demonstrates that the model can capture the macro-level variations across different geographical areas. The water use trends are further found to be flatter with less spatial heterogeneity at the prefecture scale (Figure 4 (c)). The local variations of water use cannot be reflected at the prefecture scale due to the coarser spatial resolution. Areas with stable water use, such as the northern provinces, show a more uniform distribution of water use, indicating that coarser resolution tend to mask these local variations.

The water use results at the three different spatial scales from probability rule show that the probability rule CA model can effectively capture the spatial heterogeneity in water use. The incorporation of transition probabilities and statistical distributions helps account for the temporal water use variations. However, water uses in the areas with experiencing rapid changes show great fluctuations and spatial fragmentation, and they are hard to be simulated by the probability rule. As the linear rule CA model can provide a more stable alternative in rapid change areas, it can be implemented in water use simulation, too.

4.1.2 Water use simulation from linear rule CA model

There are three parameters to be calibrated in the linear rule CA model: the self-influence coefficient α, the neighboring influence coefficient β, and the spatial decay exponent p. The dataset from 1998–2009 is for calibrating the model while the dataset from 2010–2013 is for its validation. And *RMSE* and *RE* are taken as the performance evaluation metrics. After minimizing the *RMSE* and *RE* metrics, the three optimal parameter values of the model at the three different scales are illustrated in Figure 5.

https://doi.org/10.5194/egusphere-2025-2734
Preprint. Discussion started: 27 June 2025

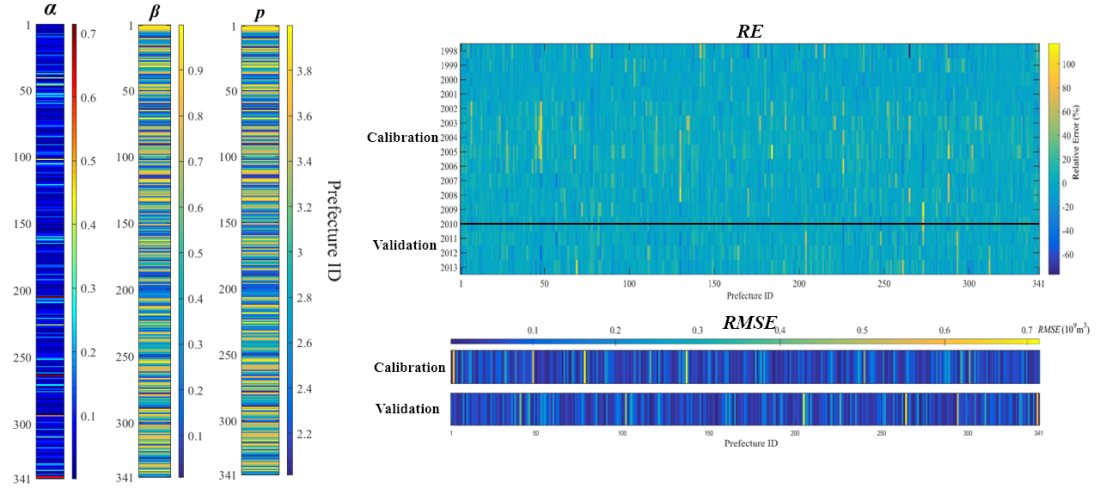

(a)

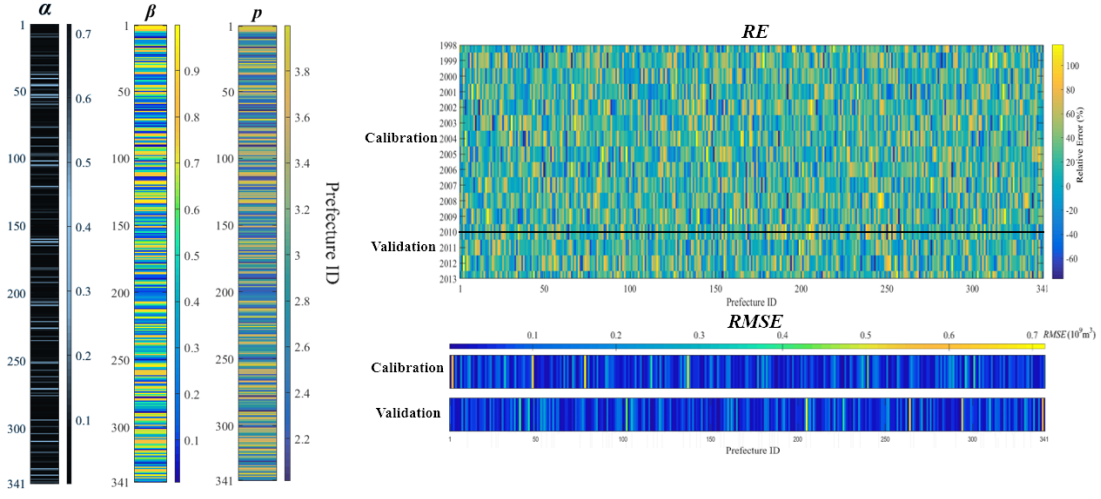

(b)

https://doi.org/10.5194/egusphere-2025-2734
Preprint. Discussion started: 27 June 2025

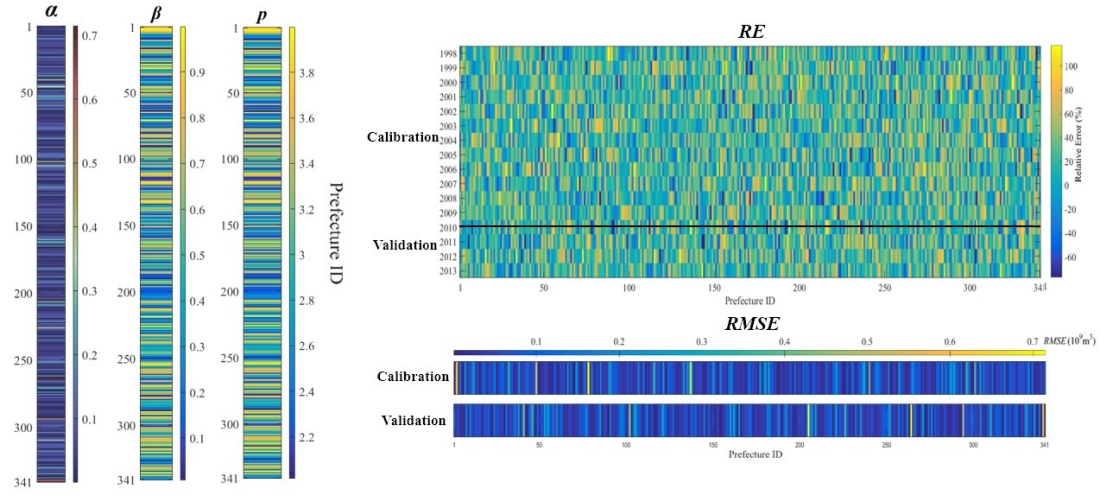

(c)

Figure 5. Optimal parameters of the linear rule CA model and the model performances at: (a) 1km scale; (b) appropriate spatial scale; (c) prefecture scale

According to the results as shown in Figure 5, the calibrated parameters are varied with scales and the performances of the models are acceptable. The spatial heterogeneity of the parameters α, β, and p tend to reflect local water use patterns. There is a balance between α and β in the areas with lower *RMSE* and *RE* values from the results at 1 km scale as shown in Figure 5(a). And both self-dependence and spatial diffusion jointly govern stable and reliable simulations. But at the appropriate spatial scale (Figure 5 (b)), the parameter values show their deviations from those of the 1 km scale, and α and β values become more regionally specific. As β plays a more dominant role in every prefecture, and higher *RMSE* and *RE* values are found. So only heavily spatial diffusion may fail to capture the complexities of local water use dynamics. These areas often experience a more varied water use. At the prefecture scale (Figure 5 (c)), the parameters are more likely to be dominated by α, especially in regions with large-scale infrastructure or agricultural variations. Their simulation errors are higher because the spatial variations are more difficult to be captured at this prefecture coarser resolutions. And the influence of β tends to be lower at this scale.

https://doi.org/10.5194/egusphere-2025-2734
Preprint. Discussion started: 27 June 2025

After calibrating the parameters for the linear rule of CA model, the water use grid maps for the period 1998–2013 are obtained and their simulated water use maps from 1998 to 2013 are also illustrated in Figure 6 at three scales (i.e., 1km scale, appropriate spatial scale and prefecture scale).

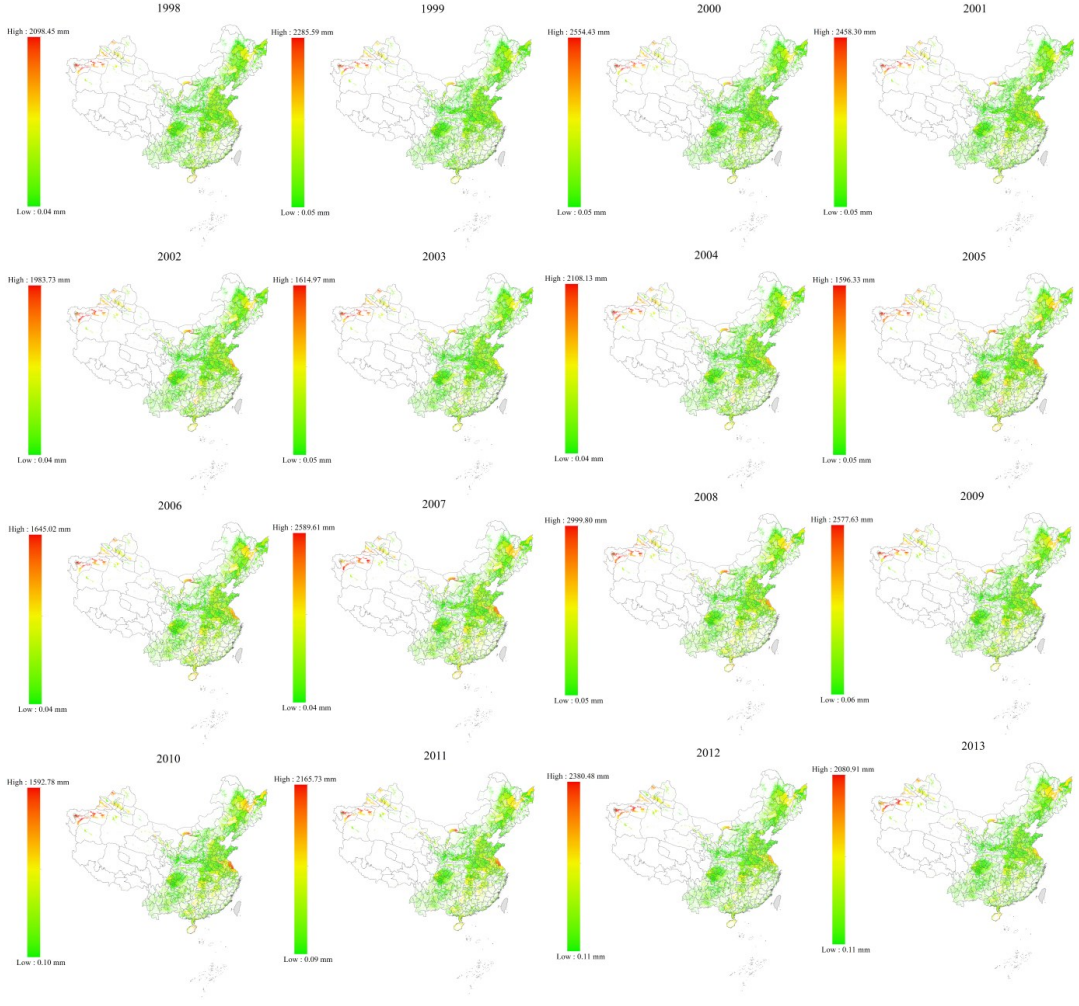

(a)

https://doi.org/10.5194/egusphere-2025-2734
Preprint. Discussion started: 27 June 2025

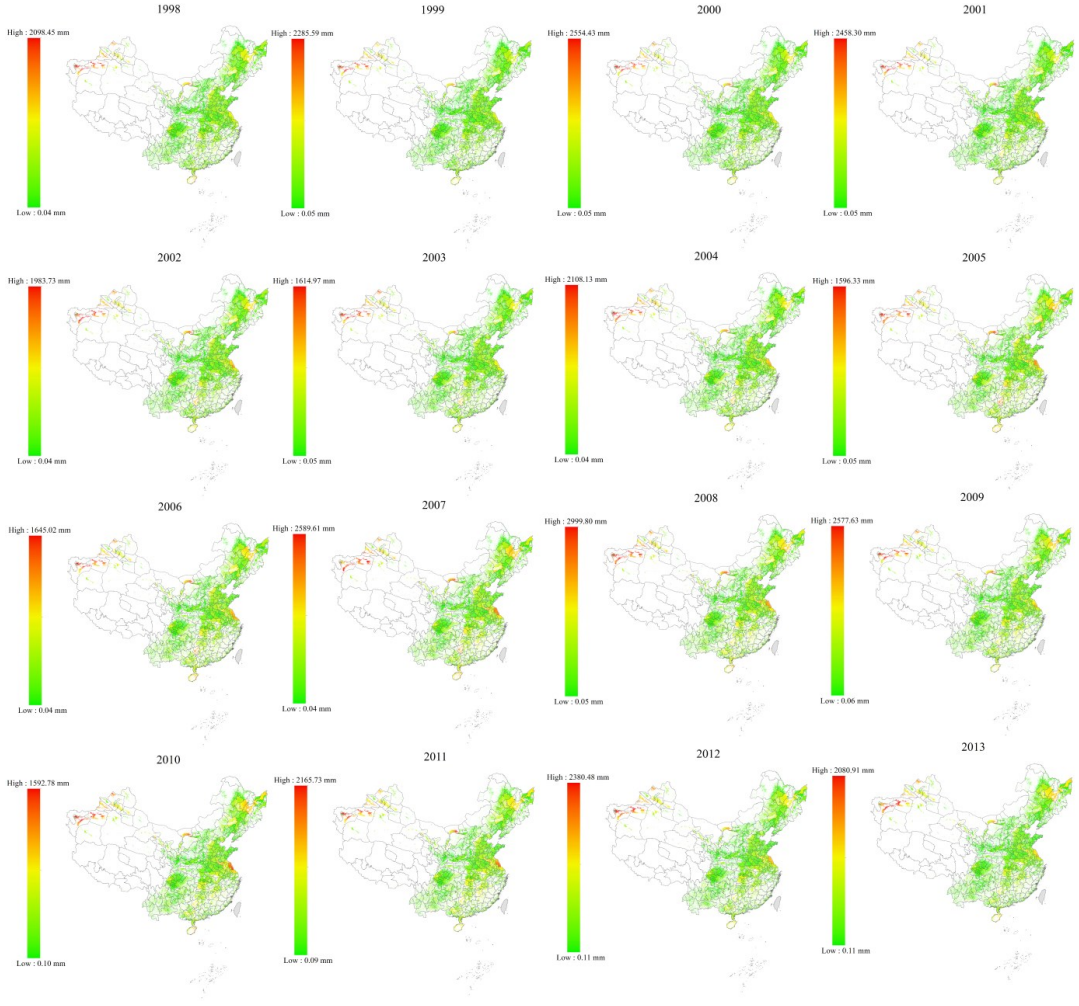

367
368 (b)

https://doi.org/10.5194/egusphere-2025-2734
Preprint. Discussion started: 27 June 2025

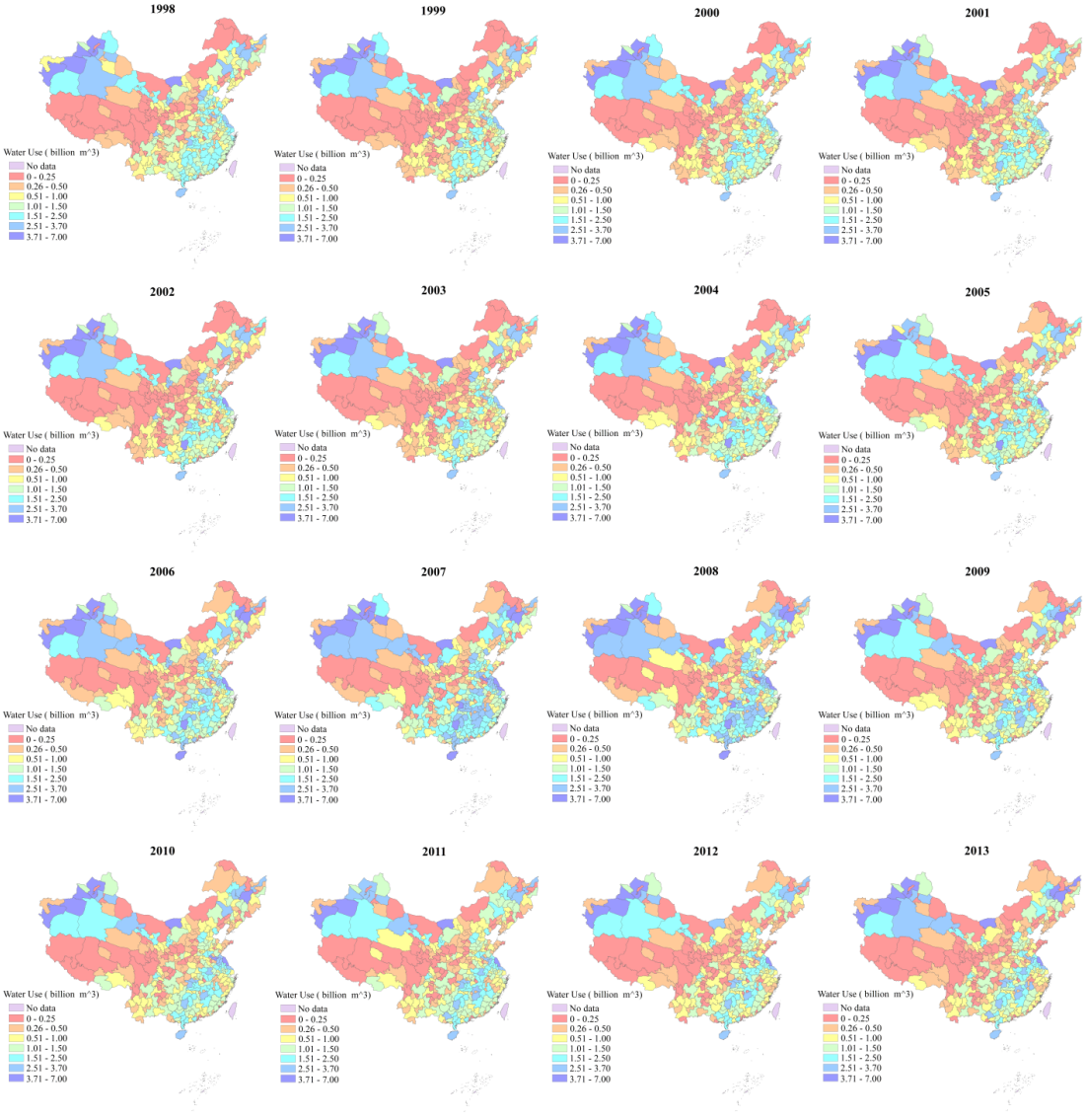

(c)

Figure 6. Water use simulation results from the linear rule at three different scales: (a) 1km scale; (b) appropriate spatial scale; (c) prefecture scale

The simulated water use maps of the linear rule from 1998 to 2013 are shown in Figure 6, and they exhibit clear spatial dynamics at different spatial scales. At the 1 km scale (Figure 6 (a)), the maps reveal the fine-scale variations in water use, highlighting their localized hotspots of high-water use, particularly in

https://doi.org/10.5194/egusphere-2025-2734
Preprint. Discussion started: 27 June 2025

economically developed urban centers such as the Yangtze River Delta, the Pearl River Delta, and the Beijing–Tianjin–Hebei region. There are upward trends, which aligns with the patterns of population growth, industrial expansion, and urbanization. From the results at the appropriate spatial scale as shown in Figure 6 (b), the localized variations in water use are captured with more clarity and precision. The appropriate scale provides a balanced representation that captures both the fine-scale dynamics and broader regional trends. At the prefecture scale (Figure 6 (c)), the water use patterns become more smoothed. This bigger resolution limits the model's ability to capture the dynamics even though the general upward trend in water use in urbanized regions is still observable. The localized fluctuations or abrupt changes driven by specific local policies or external factors are not fully represented at these bigger scales.

The simulation results across three different spatial scales can also indicate the impacts of scale on perceived water use. Finer-resolution maps reveal localized hotspots of high water use that can be averaged out in coarser resolution. It demonstrates that the CA model's flexibility and further confirms the importance of multi-scale analysis in understanding water use.

4.2 Uncertainty estimation of water use simulation from GLUE

To further assess the reliability and robustness of the water use simulations from the CA model, the uncertainty is quantified by GLUE. According to the calibrated parameters for the probability and linear rules, the uncertainty ranges of the model outputs across different spatial scales are obtained through GLUE. To figure out both the accuracy of simulations and the confidence levels of model predictions from the parameter uncertainties, ensembles of the parameters combination were generated by the uniform sampling as the description in Section 2.3. Corresponding results from the CA model were obtained and their performances are quantified by *RMSE* and *RE* metrics. If the *RMSE* and *RE* metrics are acceptable according to their pre-defined thresholds, the maximum and minimum of the simulation results from the CA model are taken as their

https://doi.org/10.5194/egusphere-2025-2734
Preprint. Discussion started: 27 June 2025

398 uncertainty range. These uncertainties across the three spatial scales are shown in Figure 7 from the probability
399 rule and in Figure 8 from the linear rule at the 95% confidence level (i.e., pre-defined threshold). These
400 uncertainties are from the parameter variabilities. A wider range of the uncertainties indicates lower stable and
401 reliable simulation results, while narrower ones suggest stable and reliable simulation results. The spatial
402 variation of uncertainty ranges can also reveal the significant regional differences of the simulations at
403 different spatial resolutions.

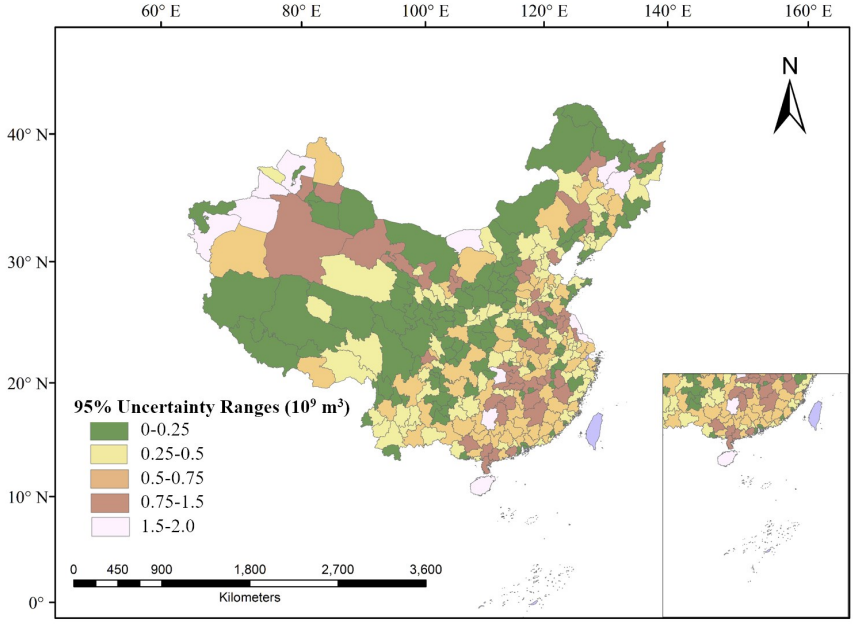

404
405 (a)

https://doi.org/10.5194/egusphere-2025-2734
Preprint. Discussion started: 27 June 2025

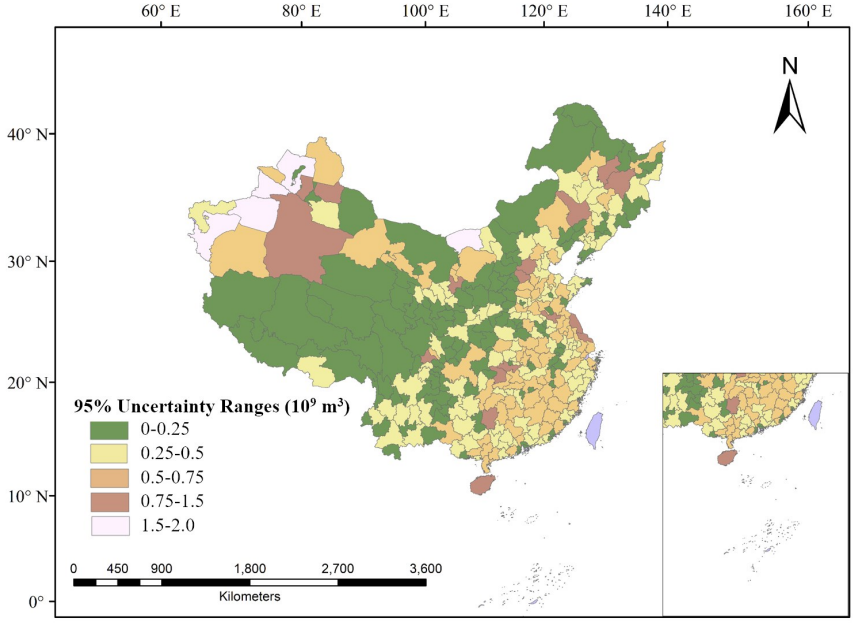

(b)

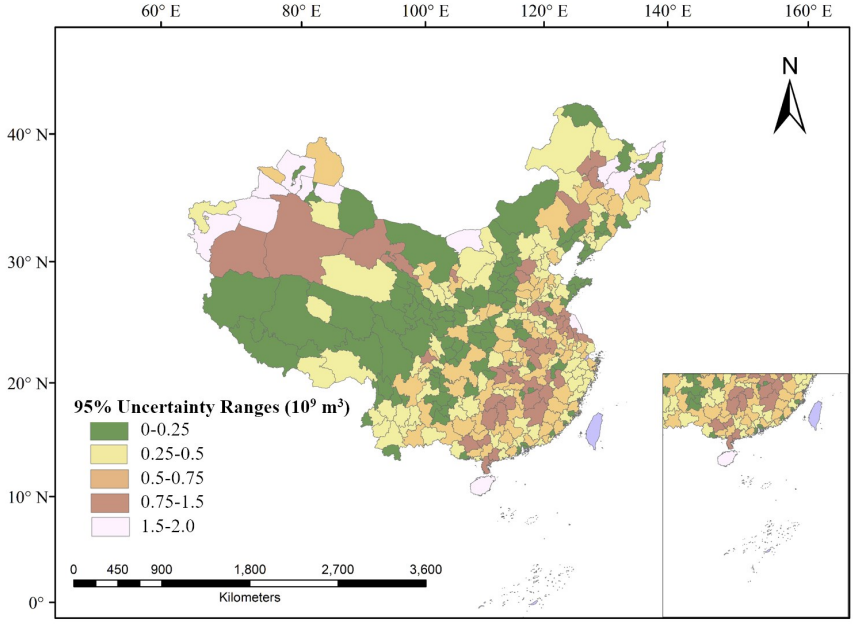

(c)

Figure 7. The uncertainty ranges of water use simulations at the 95% confidence level at three spatial scales from the probability rule at: (a) 1km scale; (b) appropriate spatial scale; (c) prefecture scale

https://doi.org/10.5194/egusphere-2025-2734
Preprint. Discussion started: 27 June 2025

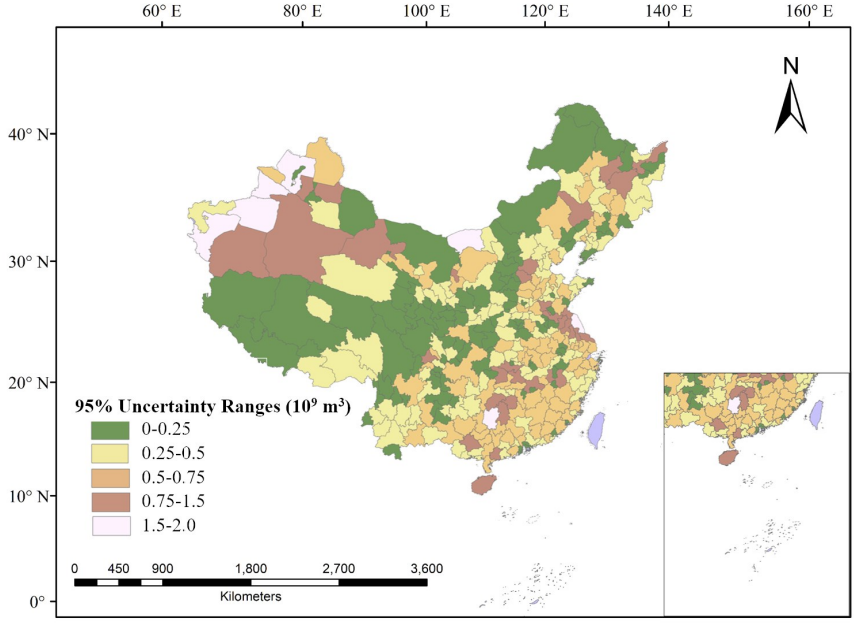

412
413 (a)

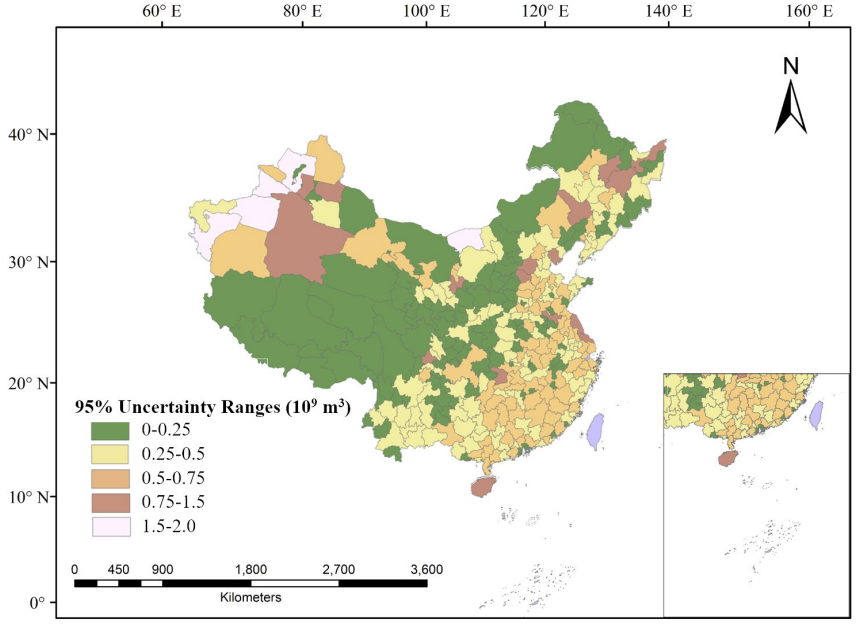

414
415 (b)

https://doi.org/10.5194/egusphere-2025-2734
Preprint. Discussion started: 27 June 2025

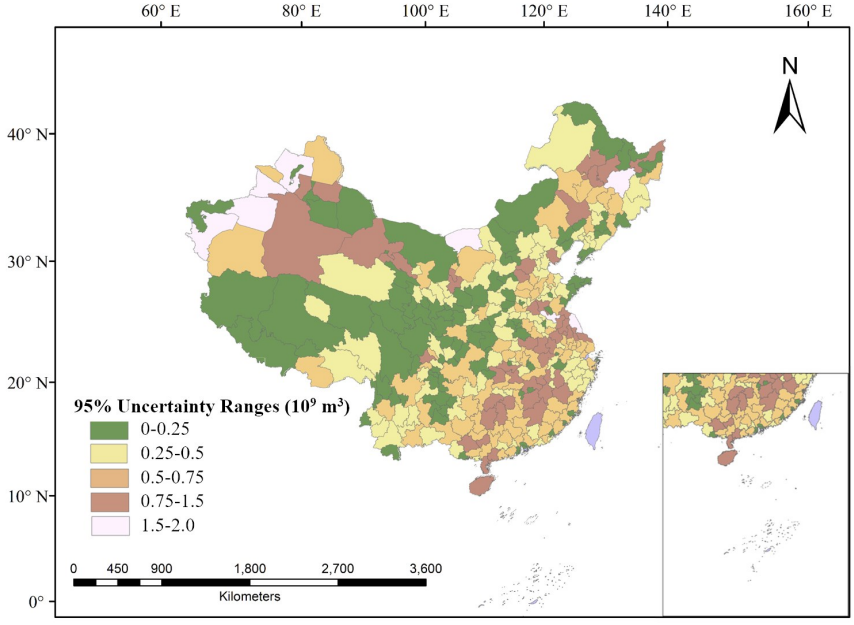

(c)

Figure 8. The uncertainty ranges of water use simulations at the 95% confidence level at three spatial scales based on linear rule at: (a) 1km scale; (b) appropriate spatial scale; (c) prefecture scale

There are distinct regional patterns of simulation uncertainty from the spatial distribution of the uncertainty ranges at the 95% confidence level. Larger uncertainty ranges (i.e., 0.75–2.0*$10^9 m^3$) are predominantly found in western and southwestern prefectures, such as Xinjiang, Qinghai, Gansu, and Chongqing, where data scarcity and complex local dynamics likely contribute to higher model uncertainty. In contrast, most eastern and northeastern regions, including Beijing, Jiangsu, Shandong, and Liaoning, exhibit relatively narrow uncertainty ranges (i.e., 0–0.5*$10^9 m^3$), indicating more stable historical water use behavior and better alignment with CA model assumptions.

The model for the higher spatial resolutions has been found to be more sensitive to the local variations, and its uncertainty can be amplified in heterogeneous land use or socio-economic condition areas. For instance, large uncertainty ranges can be found in the densely populated urban centers or the regions undergoing rapid

https://doi.org/10.5194/egusphere-2025-2734
Preprint. Discussion started: 27 June 2025

industrialization at the 1 km scale as shown in Figure 7 (a) and Figure 8 (a). But small uncertainty ranges can be found in the same areas from the coarser-scale simulations due to the averaging of the localized fluctuations as seen in Figure 7 (c) and Figure 8 (c) at the prefecture scale. However, the small uncertainty ranges are obtained at the cost of masking the sub-regional dynamics. There should be trade-off between capturing detail and maintaining stability. Thus, it is important to select an appropriate spatial scale for the specific planning or policy purposes.

The larger uncertainty ranges are more common from the probability rule than those from the linear rule, particularly in regions with complex or highly variable water use patterns. This is largely attributed to the probability rule itself, because there are randomness in both state transitions and value sampling in fitting distributions. Although the probability rule can help the model to capture non-linear dynamics and abrupt changes, it brings higher uncertainty into outputs. In contrast, the linear rule generally brings less uncertainty, reflecting the deterministic structure of its update mechanism in the model. The amount of water use in each cell is predicted by the weighted influences from itself and neighboring cells. In regions with relatively stable and spatially smooth development patterns, such as the eastern and northeastern parts of China, the linear rule is more effective. However, the linear rule's assumption of gradual spatial continuity fails to capture abrupt local changes in the rapidly changing or the weak spatial correlation water use areas—such as Fujian, Chongqing, and some parts of Guizhou and Sichuan. And the linear rule potentially leads to an underestimation of uncertainty.

To further examine the temporal dynamics and regional differences in model uncertainty, Daqing, Chongqing, Fuzhou, Kashgar, Ningbo, and Bayannur are selected as six representative prefectures according to their geographic locations, socio-economic conditions, and water use behaviors. The time series of 95% uncertainty ranges from 1998 to 2013 for each representative prefecture is obtained from the results of the

https://doi.org/10.5194/egusphere-2025-2734
Preprint. Discussion started: 27 June 2025

452 probability and linear update rules at different spatial scales, illustrated as Figure 9.

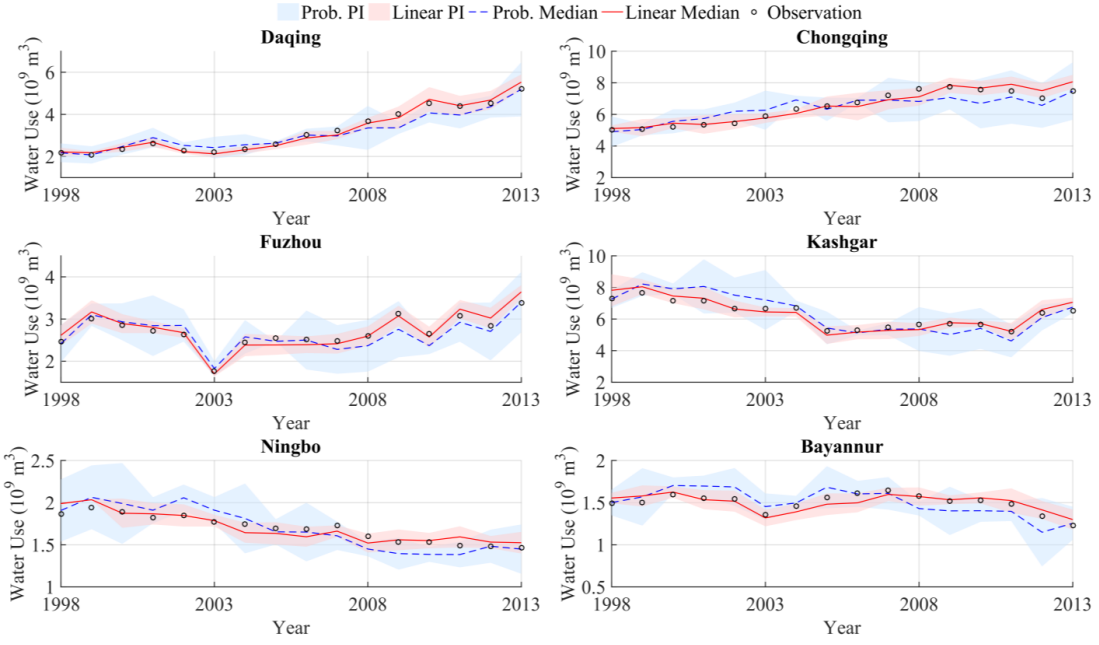

453

454 (a)

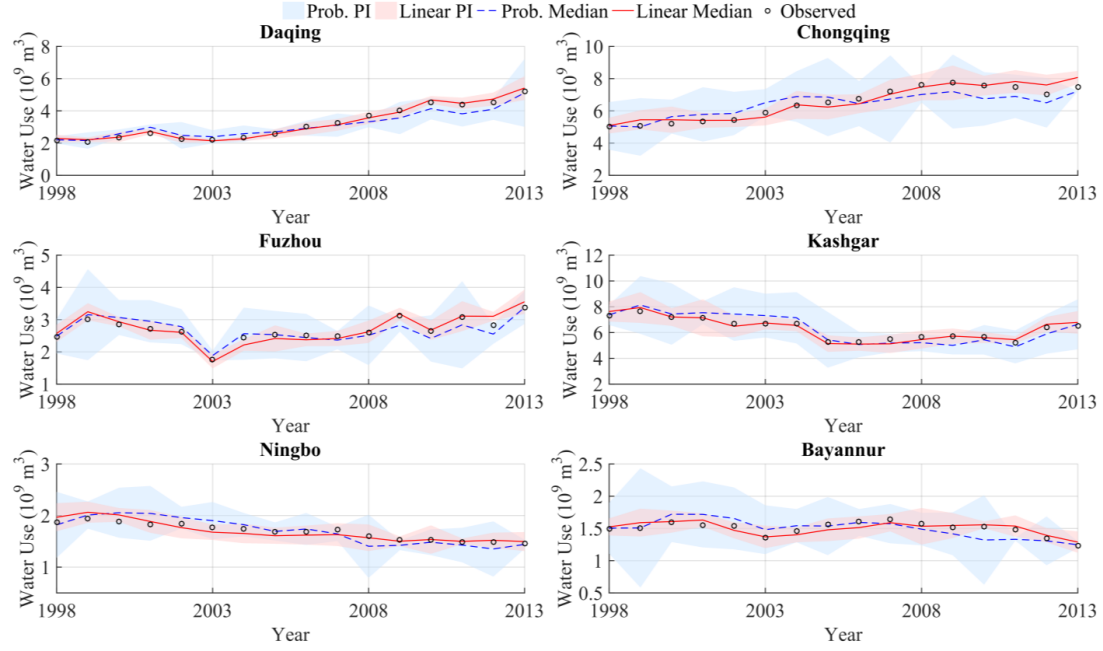

455

456 (b)

https://doi.org/10.5194/egusphere-2025-2734
Preprint. Discussion started: 27 June 2025

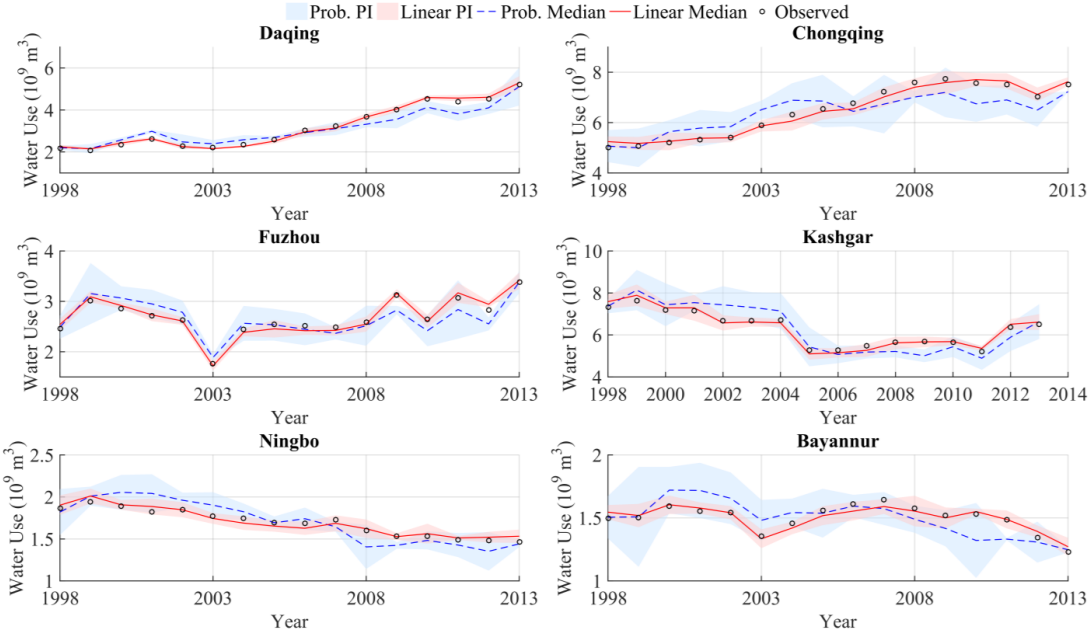

(c)

Figure 9. Time series of 95% uncertainty ranges from 1998 to 2013 for each representative prefecture from both the probability and linear update rules at different spatial scales: (a) 1km scale; (b) appropriate spatial scale; (c) prefecture scale

There is distinct the patterns across the selected prefectures as shown in Figure 9. The results from the probability rule have been found to be consistently wider uncertainty intervals than that from the linear rule, particularly in prefectures with more unstable water use conditions. For instance, Kashgar and Bayannur that are located in arid and less-developed western regions exhibit larger and more variable uncertainty intervals from the probability rule. And they are results of the combined effects of high inter-annual variability and limited input data. In contrast, Ningbo and Daqing that are located in the more stable water use trends and better data coverage areas have been found to show relatively narrow and consistent uncertainty from both two rules. It is also interesting to find that the moderate uncertainty levels with obvious differences between the two rules have been in Chongqing and Fuzhou with too many transitional urban areas. As the rapid

https://doi.org/10.5194/egusphere-2025-2734
Preprint. Discussion started: 27 June 2025

urbanization and economic shifts bring the localized instability, the probability rule can capture the shifts whereas the linear rule can only underestimate uncertainty during periods of structural change due to its lower sensitivity.

Beside the temporal and rule-based variability, the spatial scale size also plays a crucial role in shaping simulation uncertainty. With the spatial resolution of the model increases, the simulation uncertainty tends to increase, especially in regions with high spatial heterogeneity, such as arid or rapidly developing areas. The finer resolutions can effectively capture the localized variations in water use, there are higher levels of uncertainty due to the increased sensitivity to local fluctuations. In contrast, the results at coarser resolutions tend to be smoothed these local variations, there will be narrower uncertainty but potentially overlooking the sub-regional dynamics.

The uncertainty results have highlighted the importance of the spatial and temporal variations for evaluating the simulation model performance and uncertainty. The results of the representative six prefectures suggest that there is no one single update rule can outperform the others. Instead, the most appropriate rule depends on the local water use dynamics and the purpose of the water use simulation.

5 Discussion

5.1 Impacts of Update Rules on Water Use Simulation

To assess the performance of different update rules, we upscaled the simulation results at the three scales to the provincial administrative level and obtained the *RMSE* and *RE* metrics from both the probability and linear update rules. There are notable differences of the results from the two update rules as summarized in Table 2.

https://doi.org/10.5194/egusphere-2025-2734
Preprint. Discussion started: 27 June 2025

492 Table 2. Model performance at the provincial administrative level from different update rules

Provinces	*RMSE* (billion m^3)		*RE* (%)	
	Linear rule	Probability rule	Linear rule	Probability rule
Beijing	0.03	0.05	+12	+19
Tianjin	0.02	0.02	-11	-17
Shanghai	0.02	0.04	-13	-25
Chongqing	0.04	0.07	+16	+17
Anhui	0.12	0.17	+23	+32
Fujian	0.17	0.21	-23	+37
Gansu	0.35	0.43	+27	+29
Guangdong	0.26	0.36	+21	+32
Guizhou	0.31	0.40	-26	-34
Hainan	0.11	0.21	-12	+19
Heilongjiang	0.42	0.37	-27	+24
Hunan	0.21	0.11	-16	+10
Jilin	0.36	0.43	+28	+25
Jiangsu	0.12	0.17	-12	-26
Jiangxi	0.22	0.26	+24	-31
Inner Mongolia	0.19	0.29	-23	-35
Qinghai	0.31	0.41	+43	+36
Ningxia	0.11	0.20	-31	-41
Shandong	0.21	0.36	+29	-36
Shanxi	0.42	0.61	+31	+42
Shannxi	0.27	0.43	-32	-39
Sichuan	0.39	0.41	+31	+46
Xizang	0.56	0.61	-62	-79
Xinjiang	0.68	0.72	+69	+83
Yunnan	0.25	0.34	-37	-47
Zhejiang	0.21	0.29	+18	+12
Guangxi	0.34	0.42	-32	-39

https://doi.org/10.5194/egusphere-2025-2734
Preprint. Discussion started: 27 June 2025

Hubei	0.29	0.39	+27	+26
Liaoning	0.35	0.41	+33	+48

The results from the linear rule have been found to performance better than that from the probability rule in terms of its lower *RMSE* and *RE* values. The differences between the results from the two update rules are based on their update mechanisms. The design distribution-based state transitions are stochasticity in the probability rule. It can capture uncertainty in terms of the abrupt or nonlinear changes in water use while it can also bring the potential divergences from the observed trends, especially when data are sparse or when local variability is high. As a result, several higher *RMSE* and *RE* values had been found, particularly those characterized by complex topography or heterogeneous socio-economic development patterns. In contrast, the linear rule employs a deterministic update process based on local spatial averages, which tends to smooth out their fluctuations and enhance stability. In other words, the heterogeneous socio-economic development patterns have inherently been smoothed for reducing the local-level variability by the linear rule at the provincial scale. The differences of their performance from the two rules are particularly noticeable in inland or in less urbanized provinces, where the probability rule's flexibility amplifies the uncertainties.

5.2 Impact of Spatial Scales on Water Use Simulation

To investigate how spatial resolution influences the accuracy of the water use simulation, their performances at the three spatial scales (i.e., 1 km scale, appropriate intermediate scale, and prefecture scale) are evaluated and are aggregated to the provincial level to ensure comparability across scales. Their results are summarized in Table 3 and indicate their notable differences in simulating accuracy depending on its spatial scales.

https://doi.org/10.5194/egusphere-2025-2734
Preprint. Discussion started: 27 June 2025

513 Table 3. Model performance at the provincial administrative level at different spatial scales

Provinces	*RMSE* (billion m^3)			*RE* (%)		
	1 km scale	Appropriate scale	Prefecture scale	1 km scale	Appropriate scale	Prefecture scale
Beijing	0.04	0.03	0.05	+22	+12	+19
Tianjin	0.04	0.02	0.06	+26	-11	-17
Shanghai	0.03	0.02	0.04	-23	-13	-25
Chongqing	0.06	0.04	0.07	-26	+16	+27
Anhui	0.17	0.12	0.19	+35	+23	+32
Fujian	0.23	0.17	0.21	-31	-23	+37
Gansu	0.41	0.35	0.43	+31	+27	+29
Guangdong	0.31	0.26	0.36	-29	+21	+32
Guizhou	0.36	0.31	0.40	+31	-26	-34
Hainan	0.19	0.11	0.21	+16	-12	+19
Heilongjiang	0.49	0.42	0.47	+31	-27	+34
Hunan	0.26	0.21	0.31	-19	-16	+20
Jilin	0.42	0.36	0.43	-31	+28	+35
Jiangsu	0.19	0.12	0.17	-21	-12	-26
Jiangxi	0.31	0.22	0.36	-26	+24	-31
Inner Mongolia	0.26	0.19	0.29	-31	-23	-35
Qinghai	0.40	0.31	0.41	+52	+43	+56
Ningxia	0.21	0.11	0.30	-39	-31	-41
Shandong	0.29	0.21	0.36	-32	+29	-36
Shanxi	0.53	0.42	0.61	+36	+31	+42
Shannxi	0.34	0.27	0.43	-36	-32	-39
Sichuan	0.42	0.39	0.41	+41	+31	+46
Xizang	0.67	0.56	0.61	-74	-62	-79
Xinjiang	0.79	0.68	0.72	+72	+69	+83
Yunnan	0.31	0.25	0.34	-49	-37	-47
Zhejiang	0.24	0.21	0.29	+23	+18	+32

https://doi.org/10.5194/egusphere-2025-2734
Preprint. Discussion started: 27 June 2025

Guangxi	0.39	0.34	0.42	-36	-32	-39
Hubei	0.35	0.29	0.39	+31	+27	+36
Liaoning	0.37	0.35	0.41	+42	+33	+48

The relatively lower accuracy of the 1 km scale simulations is attributed to the increased sensitivity to local heterogeneity. At the 1km scale, small errors from the input variables or local noise can accumulate and amplify to larger discrepancies. Although the results from1kmscale take more spatial detail to reflect the variations in water use, it also brings the uncertainty, especially in the regions with the fragmented data or the high socio-economic diversity. The simulation results from the prefecture level tend to oversimplify the spatial variation. Generally, the results from the coarse resolution have smoothed the intra-regional differences in water use patterns, and resulted in under or over-predictions at the provincial administrative level. The reduced spatial granularity leads to reduction in uncertainty of simulation but can mask the disparities that are critical to policy implementation and resource allocation.

The results from the appropriate scale can balance the spatial sensitivity and model stability. It is fine enough to capture meaningful spatial heterogeneity, and it is yet coarse enough to mitigate excessive noise and data sparsity effects. The most reliable simulating water use should be based on this scale. And it should be noted that that it is crucial for improving simulation reliability to select an appropriate spatial resolution that aligns with both the model structure and the scale of decision-making.

5.3 Spatial Heterogeneity of Water Use Grid Maps

To understand the variation of the spatial heterogeneity of water use, the Coefficient of Variation (CV) and Moran's I were used to quantify the degree of variability and spatial autocorrelation of water use across at three different spatial scales across the study area.

The highest CV values have been found in the results of water use simulation at the 1 km scale among

https://doi.org/10.5194/egusphere-2025-2734
Preprint. Discussion started: 27 June 2025

the three scales. There are the most significant regional differences at the 1 km scale. As Moran's I can reveal the positive autocorrelation that suggests the clustering of high or low water use. The results of Moran's I analysis at the 1 km scale show that there is a strong pattern of spatial dependence in urban areas, particularly in regions with intense agricultural or industrial water use.

Different from the results from the 1 km scale, the results from the appropriate scale show the decreasing water use heterogeneity with lower CV values. As more local variations are captured by the smaller scale grid, the bigger named appropriate scale here can balance the capturing regional heterogeneity and the reducing excessive spatial details for water us simulation. And there are also positive autocorrelations with Moran's I values at the appropriate scale even with less degree of clustering.

It is no doubt that the lowest spatial heterogeneity of water use simulation have been found with the lowest CV values at the prefecture scale. The regional variations of water use data at larger spatial scales are often smoothed out. The moderate positive autocorrelation of Moran's I values indicate that while there is still spatial dependence, it is less distinct compared to finer scales.

It is suggested that the spatial scale of the water use simulation significantly impacts the representation of spatial heterogeneity. The results from 1 km scale can capture the most detailed variability, while the appropriate scale provides a more balanced view of spatial heterogeneity, and the prefecture scale tends to generalize water use patterns, reducing the granularity of spatial differences.

6 Conclusion

A multi-scale water use simulation framework has been proposed through integrating a CA model with GLUE to address spatial heterogeneity and uncertainty in this study. Both probability rule and linear rule across three spatial scales (i.e., 1 km, appropriate scale, and prefecture scale) have been applied over 341 prefectures in China as a case study. The impacts of model structure and spatial scale on the spatial

https://doi.org/10.5194/egusphere-2025-2734
Preprint. Discussion started: 27 June 2025

heterogeneity and uncertainty have been figured out.

It is interesting to find that the probability rule effectively captures stochastic variations and abrupt transitions in water use but brings larger uncertainty due to its random sampling nature. And the linear rule brings more stable and accurate simulations, particularly in regions with smoother water use patterns. The local noise and uncertainty tend to be amplified in the results of the water use simulation at the 1km scale , while the essential spatial heterogeneity tend to be oversimplified and suppressed in the results at the prefecture scale The most reliable simulation are found from the appropriate scale due its trade-off between capturing spatial heterogeneity and maintaining model stability.

Future improvements for the water use simulation should involve the adaptive update rules that respond to external drivers such as policy shifts or climate shocks, and extend the simulation to finer temporal scales (e.g., seasonal or monthly) for improved short-term decision making. More uncertainty quantification methods, such as Bayesian inference or Markov Chain Monte Carlo, are recommended to enhance performance in high-dimensional settings. Overall, our study can contribute to the water use simulation at a multi-scale and with uncertainty-aware. Our proposed framework will be helpful for the integrated water management, infrastructure planning, and environmental policy under changing socio-economic and climatic conditions.

https://doi.org/10.5194/egusphere-2025-2734
Preprint. Discussion started: 27 June 2025

Author contributions

JZ designed the model architecture, performed the computations, conducted the statistical analysis, and drafted the manuscript. DL acquired funding, contributed to the study design, provided research data, supervised the project, and guided the manuscript revision. JW contributed to manuscript revision discussions and provided advice on submission procedures. FU, LX, ZP, and WG participated in revision discussions and contributed to figure and chart preparation. All authors reviewed and approved the final version of the manuscript for submission.

Competing interests

The authors declare that they have no conflict of interest.

Acknowledgement

The authors gratefully acknowledge the financial support from National Key R&D Program of China (2024YFC3012402 and 2022YFC3202803), the National Natural Science Foundation of China (Nos.52379022, and 51879194).

https://doi.org/10.5194/egusphere-2025-2734
Preprint. Discussion started: 27 June 2025

References

Abdi H. Coefficient of variation. Encycl. Res. Des., 1(5), 169–171, https://doi.org/10.4135/9781412961288.n56, 2010.

Al-Shaar, W., Nehme, N., Haidar, H. and Lakiss, H. Forecasted water demand using Extended Cellular Automata Markov Chain Model: case of Saida and Jezzine regions in Lebanon, Sustain. Water Resour. Manag., 8(3), 71, https://doi.org/10.1007/s40899-022-00656-7, 2022.

Almino, L.M.D. and Rufino, I.A.A. Dynamic modeling and urban water demand scenarios: simulations in Campina Grande-PB, Eng. Sanit. Ambient., 26, 915–925, https://doi.org/10.1590/S1413-415220190015, 2021.

Avargani, H.K., Shahdany, S.M.H., Kamrani, K., Maestre, J.M., Garmdareh, S.E.H. and Liaghat, A. Prioritization of surface water distribution in irrigation districts to mitigate crop yield reduction during water scarcity, Agric. Water Manag. 269, 107653, https://doi.org/10.1016/j.agwat.2022.107653, 2022.

Botta-Dukát, Z.J.S.R. Quartile coefficient of variation is more robust than CV for traits calculated as a ratio, Sci. Rep., 13(1), 4671, https://doi.org/10.1038/s41598-023-31306-9, 2023.

Brunner, M.I., Zappa, M. and Stähli, M. Scale matters: Effects of temporal and spatial data resolution on water scarcity assessments, Adv. Water Resour., 123, 134–144, https://doi.org/10.1016/j.advwatres.2018.12.001, 2019.

Canchola, J., Tang, S., Hemyari, P., Paxinos, E. and Marins, E.J.M.P.B. Correct use of percent coefficient of variation (CV) formula for log-transformed data, MOJ Proteom. Bioinform., 6(4), 316–317, https://doi.org/10.15406/mojpb.2017.06.00200, 2017.

Cao, X., Wu, M., Zheng, Y., Guo, X., Chen, D. and Wang, W. Can China achieve food security through the development of irrigation ? , Reg. Environ. Change, 18(2), 465–475, https://doi.org/10.1007/s10113-017-1214-5, 2018.

Carvalho, T.M.N., Filho, F.d.A.d.S. and Porto, V.C. Urban Water Demand Modeling Using Machine Learning Techniques: Case Study of Fortaleza, Brazil, J. Water Resour. Plan. Manag., 147(1), 05020026, https://doi.org/10.1061/(ASCE)WR.1943-5452.0001196, 2021.

Chen, J., Brissette, F.P. and Leconte, R. Uncertainty of downscaling method in quantifying the impact of climate change on hydrology, J. Hydrol., 401(3), 190–202, https://doi.org/10.1016/j.jhydrol.2011.02.020, 2011.

Dolan, F., Lamontagne, J., Link, R., Hejazi, M., Reed, P. and Edmonds, J. Evaluating the economic impact of water scarcity in a changing world, Nat. Commun., 12(1), , https://doi.org/10.1038/s41467-021-21668-4, 2021.

Fu, Q., Zhou, M., Li, Y., Ye, X., Yang, M. and Wang, Y.J.G.A. Flow spatiotemporal Moran's I: Measuring the spatiotemporal autocorrelation of flow data, Geogr. Anal., 56(4), 799–824, https://doi.org/10.1111/gean.12397, 2024.

Galelli, S. and Castelletti, A. Tree-based iterative input variable selection for hydrological modeling, Water Resour. Res., 49(7), 4295–4310, https://doi.org/10.1002/wrcr.20481, 2013.

Gedamu, W.T., Plank-Wiedenbeck, U., Wodajo, B.T.J.A.A. and Prevention. A spatial autocorrelation analysis of road traffic crash by severity using Moran's I spatial statistics: A comparative study of Addis Ababa and Berlin cities, Accid. Anal. Prev., 200, 107535, https://doi.org/10.1016/j.aap.2024.107535, 2024.

Guevara, M. and Vargas, R. Downscaling satellite soil moisture using geomorphometry and machine learning, PLoS ONE, 14(9), e0222590, https://doi.org/10.1371/journal.pone.0222590, 2019.

He, S.K., Guo, S.L., Liu, Z.J., Yin, J.B., Chen, K.B. and Wu, X.S. Uncertainty analysis of hydrological multi-model ensembles based on CBP-BMA method, Hydrol. Res., 49(5), 1636–1651, https://doi.org/10.2166/nh.2017.248, 2018.

Hersbach, H., Bell, B., Berrisford, P., Hirahara, S., Horányi, A., Muñoz-Sabater, J., Nicolas, J., Peubey, C., Radu, R., Schepers, D., Simmons, A., Soci, C., Abdalla, S., Abellan, X., Balsamo, G., Bechtold, P., Biavati, G., Bidlot, J., Bonavita, M., De Chiara, G., Dahlgren, P., Dee, D., Diamantakis, M., Dragani, R., Flemming, J., Forbes, R., Fuentes, M., Geer, A., Haimberger, L., Healy, S., Hogan, R.J., Hólm, E., Janisková, M., Keeley, S., Laloyaux, P., Lopez, P., Lupu, C., Radnoti, G., de Rosnay, P., Rozum, I., Vamborg, F., Villaume, S. and Thépaut, J.-N. The ERA5 global reanalysis, Q. J. R. Meteorol. Soc., 146(730), 1999–2049, https://doi.org/10.1002/qj.3803, 2020.

Horta, A., Oliveira, A.R., Azevedo, L. and Ramos, T.B.J.G.R. Assessing the use of digital soil maps in hydrological modeling for soil-water budget simulations-implications for water management plans in southern Portugal, Geoderma Reg., 36, e00741, https://doi.org/10.1016/j.geodrs.2023.e00741, 2024.

Hou, C., Li, Y., Sang, S., Zhao, X., Liu, Y., Liu, Y. and Zhao, F. High-resolution mapping of monthly industrial water withdrawal in China from 1965 to 2020, Earth Syst. Sci. Data, 16(5), 2449–2464, https://doi.org/10.5194/essd-16-2449-2024, 2024.

https://doi.org/10.5194/egusphere-2025-2734
Preprint. Discussion started: 27 June 2025

Huang, Z., Yuan, X. and Liu, X. The key drivers for the changes in global water scarcity: Water withdrawal versus water availability, J. Hydrol., 601, 126658, https://doi.org/10.1016/j.jhydrol.2021.126658, 2021.
Ji, Y., Zuo, Q., Zhao, C., Zhang, Z. and Wu, Q.J.E.I.A.R. Measurement and decomposition of green water resource utilization efficiency across multiple water use sectors in China: A perspective on water-saving potential, Environ. Impact Assess. Rev., 112, 107806, https://doi.org/10.1016/j.eiar.2025.107806, 2024.
Kaewmai, R., Grant, T., Eady, S., Mungkalasiri, J. and Musikavong, C. Improving regional water scarcity footprint characterization factors of an available water remaining (AWARE) method, Sci. Total Environ., 681, 444–455, https://doi.org/10.1016/j.scitotenv.2019.05.006, 2019.
Kang, S., Hao, X., Du, T., Tong, L., Su, X., Lu, H., Li, X., Huo, Z., Li, S. and Ding, R. Improving agricultural water productivity to ensure food security in China under changing environment: From research to practice, Agric. Water Manag., 179, 5–17, https://doi.org/10.1016/j.agwat.2016.05.019, 2017.
Knox, J.W., Haro-Monteagudo, D., Hess, T.M. and Morris, J. Identifying Trade-Offs and Reconciling Competing Demands for Water: Integrating Agriculture Into a Robust Decision-Making Framework, Earth's Future, 6(10), 1457–1470, https://doi.org/10.1029/2018EF000905, 2018.
Kovacevic, J., Cvijetinovic, Z., Stancic, N., Brodic, N. and Mihajlovic, D. New Downscaling Approach Using ESA CCI SM Products for Obtaining High Resolution Surface Soil Moisture, Remote Sens., 12(7), https://doi.org/10.3390/rs12071119, 2020.
Liu, D., Li, X., Guo, S., Rosbjerg, D. and Chen, H. Using a Bayesian Probabilistic Forecasting Model to Analyze the Uncertainty in Real-Time Dynamic Control of the Flood Limiting Water Level for Reservoir Operation, J. Hydrol. Eng., 20(2), 04014036, https://doi.org/10.1061/(ASCE)HE.1943-5584.0000849, 2015.
Liu, D., Zhang, Y., Zhang, J., Xiong, L., Liu, P., Chen, H. and Yin, J. Rainfall estimation using measurement report data from time-division long term evolution networks, J. Hydrol., 600, 126530, https://doi.org/10.1016/j.jhydrol.2021.126530, 2021.
Liu, Y., Wang, N., Jiang, C., Archer, L. and Wang, Y. Temporal and spatial distribution of soil water and nitrate content affected by surface irrigation and fertilizer rate in silage corn fields, Sci. Rep., 10(1), 8317, https://doi.org/10.1038/s41598-020-65119-5, 2020.
Liu, Y., Zhang, J., Chen, L., Chu, H., Wang, J.Z. and Ma, L. SSAS: Spatiotemporal Scale Adaptive Selection for Improving Bias Correction on Precipitation, IEEE Trans. Cybern., 52(11), 12175–12188, doi: 10.1109/TCYB.2021.3072483, 2021.
Luo, Y., Zhang, Z., Li, Z., Chen, Y., Zhang, L., Cao, J. and Tao, F. Identifying the spatiotemporal changes of annual harvesting areas for three staple crops in China by integrating multi-data sources, Environ. Res. Lett., 15(7), 074003, https://doi.org/10.1088/1748-9326/ab9754, 2020.
Mekonnen, M.M. and Hoekstra, A.Y. Four billion people facing severe water scarcity, Sci. Adv., 2(2), e1500323, https://doi.org/10.1126/sciadv.1500323, 2016.
Noori, N. and Kalin, L. Coupling SWAT and ANN models for enhanced daily streamflow prediction, J. Hydrol., 533, 141–151, https://doi.org/10.1016/j.jhydrol.2015.12.020, 2016.
Rosa, L., Chiarelli, D.D., Rulli, M.C., Dell'Angelo, J. and D'Odorico, P. Global agricultural economic water scarcity, Sci. Adv., 6(18), eaay5552, https://doi.org/10.1126/sciadv.aay5552, 2020.
Sapino, F., Haer, T., Saiz-Santiago, P. and Pérez-Blanco, C.D. A multi-agent cellular automata model to explore water trading potential under information transaction costs, J. Hydrol., 618, 128669, https://doi.org/10.1016/j.jhydrol.2023.128669, 2023.
Sharifi, H., Roozbahani, A. and Hashemy Shahdany, S.M. Evaluating the Performance of Agricultural Water Distribution Systems Using FIS, ANN and ANFIS Intelligent Models, Water Resour. Manag., 35(6), 1797–1816, https://doi.org/10.1007/s11269-020-02685-3, 2021.
Shortridge, A. Practical limits of Moran's autocorrelation index for raster class maps. Computers Environment and Urban Systems. Computers, Comput. Environ. Urban Syst., 31(3), 362–371, https://doi.org/10.1016/j.compenvurbsys.2006.04.002, 2007.
Su, Y., Liao, S., Ren, J. and Zhao, Z.J.F.i.E.S. Research on the decoupling relationship between water resources utilization and economic development at the county scale in Qian'nan Prefecture, Guizhou Province, Front. Environ. Sci., 12, 1347652, https://doi.org/10.3389/fenvs.2024.1347652, 2024.
Sun, S., Tang, Q.H., Konar, M., Huang, Z.W., Gleeson, T., Ma, T., Fang, C.L. and Cai, X.M. Domestic Groundwater Depletion Supports China's Full Supply Chains, Water Resour. Res., 58(5), e2021WR031555, https://doi.org/10.1029/2021WR031555, 2022.
Sunkara, S.V. and Singh, R. Assessing the impact of the temporal resolution of performance indicators on optimal decisions of a water resources system, J. Hydrol., 612, 128185, https://doi.org/10.1016/j.jhydrol.2022.128185, 2022.
Taormina, R., Galelli, S., Karakaya, G. and Ahipasaoglu, S.D. An information theoretic approach to select alternate subsets of predictors for data-driven hydrological models, J. Hydrol., 542, 18–34, https://doi.org/10.1016/j.jhydrol.2016.08.034, 2016.
Tariq, A., Mumtaz, F., Majeed, M. and Zeng, X. Spatio-temporal assessment of land use land cover based on

https://doi.org/10.5194/egusphere-2025-2734
Preprint. Discussion started: 27 June 2025

trajectories and cellular automata Markov modelling and its impact on land surface temperature of Lahore district Pakistan, Environ. Monit. Assess., 195(1), 195, https://doi.org/10.1007/s10661-022-09942-9, 2023.

Tiefelsdorf, M., Boots, B.J.E. and A, P. The exact distribution of Moran's I, Environ. Plan. A, 27(6), 985–999, https://doi.org/10.1068/a270985, 1995.

Wang, C., Tang, G., Xiong, W., Ma, Z. and Zhu, S. Infrared precipitation estimation using convolutional neural network for FengYun satellites, J. Hydrol., 603, 127113, https://doi.org/10.1016/j.jhydrol.2021.127113, 2021.

Wang, T., Guo, Z., Shen, Y., Cui, Z. and Goodwin, A. Accumulation mechanism of biofilm under different water shear forces along the networked pipelines in a drip irrigation system, Sci. Rep., 10(1), 6960, https://doi.org/10.1038/s41598-020-63602-1, 2020.

Wu, B., Tian, F., Zhang, M., Piao, S., Zeng, H., Zhu, W., Liu, J., Elnashar, A. and Lu, Y. Quantifying global agricultural water appropriation with data derived from earth observations, J. Clean. Prod., 358, 131891, https://doi.org/10.1016/j.jclepro.2022.131891, 2022.

Wu, J. and Lu, J. Spatial scale effects of landscape metrics on stream water quality and their seasonal changes, Water Res., 191, 116811, https://doi.org/10.1016/j.watres.2021.116811, 2021.

Yamada, H.J.M. A new perspective on Moran's coefficient: Revisited, Math., 12(2), 253, https://doi.org/10.3390/math12020253, 2024.

Yan, J., Jia, S., Lv, A. and Zhu, W. Water Resources Assessment of China's Transboundary River Basins Using a Machine Learning Approach, Water Resour. Res., 55(1), 632–655, https://doi.org/10.1029/2018WR023274, 2019.

Yang, Y.R., Xiong, Q.Y., Wu, C., Zou, Q.H., Yu, Y., Yi, H.L. and Gao, M. A study on water quality prediction by a hybrid CNN-LSTM model with attention mechanism, Environ. Sci. Pollut. Res., 28(39), 55129–55139, https://doi.org/10.1007/s11356-021-14134-8, 2021.

Ye, Y., Huang, L., Zheng, Q., Liang, C., Dong, B., Deng, J. and Han, X. A feasible framework to downscale NPP-VIIRS nighttime light imagery using multi-source spatial variables and geographically weighted regression, Int. J. Appl. Earth Obs. Geoinf., 104, 102513, https://doi.org/10.1016/j.jag.2021.102513, 2021.

Yin, J., Guo, S., Gu, L., He, S., Ba, H., Tian, J., Li, Q. and Chen, J. Projected changes of bivariate flood quantiles and estimation uncertainty based on multi-model ensembles over China, J. Hydrol., 585, 124760, https://doi.org/10.1016/j.jhydrol.2019.124760, 2020.

Zhang, C. and Long, D. Estimating Spatially Explicit Irrigation Water Use Based on Remotely Sensed Evapotranspiration and Modeled Root Zone Soil Moisture, Water Resour. Res., 57(12), e2021WR031382, https://doi.org/10.1029/2021WR031382, 2021.

Zhang, J.Y., Liu, D.D., Guo, S.L., Xiong, L.H., Liu, P., Chen, J. and Yin, J.B. High resolution annual irrigation water use maps in China based-on input variables selection and convolutional neural networks, J. Clean. Prod., 405, 136175, https://doi.org/10.1016/j.jclepro.2023.136175, 2023.

Zhang, J., Liu, D., Xu, Y., Xiong, L., Chen, J., Chen, H., & Yin, J. Appropriate spatiotemporal scale selection for water use simulation in China, J. Hydrol., 2025, 133502, https://doi.org/10.1016/j.jhydrol.2024.133502, 2025.

Zhou, F., Bo, Y., Ciais, P., Dumas, P., Tang, Q.H., Wang, X.H., Liu, J.G., Zheng, C.M., Polcher, J., Yin, Z., Guimberteau, M., Peng, S.S., Ottle, C., Zhao, X.N., Zhao, J.S., Tan, Q., Chen, L., Shen, H.Z., Yang, H., Piao, S.L., Wang, H. and Wada, Y. Deceleration of China's human water use and its key drivers, Proc. Natl. Acad. Sci. U.S.A., 117(14), 7702–7711, https://doi.org/10.1073/pnas.1913587117, 2020.